Heliyon 8 (2022) e12298

Contents lists available at ScienceDirect

Heliyon

journal homepage: www.cell.com/heliyon

Research article

Seasonal land use/land cover change and the drivers in Kafta Sheraro national park, Tigray, Ethiopia

Fitsum Temesgen [a,*], Bikila Warkineh [b], Alemayehu Hailemicael [c]

[a] Center for Environmental Sciences (Environmental Resources Conservation and Management), Addis Ababa University, P.O. Box: 1176, Addis Ababa, Ethiopia
[b] Plant Biology and Biodiversity Management and Environmental Sciences, Addis Ababa University, P.O. Box: 1176, Addis Ababa, Ethiopia
[c] College of Natural Science, Arba Minch University, P.O. Box: 21, Arba Minch, Ethiopia

ARTICLE INFO

Keywords:
Land use/land cover change
Kafta Sheraro national park
Landsat
NDVI
Drivers

ABSTRACT

Kafta Sheraro National Park (KSNP) has experienced rapid and consecutive destruction of dry woodland vegetation due to the influence of anthropogenic activities in the past three decades. However, to date, the change in woodland cover and its driving factors have not been addressed. This study aims to assess the spatial and temporal trends of land use/land cover change, seasonal vegetation cover change via the normalized difference vegetation index (NDVI), and human-induced drivers of change that occurred in the KSNP between 1988 and 2018 by using satellite imagery sensors (TM, ETM$^{+,}$ OLI), field observations, and local community interview data. The 2018 image results showed kappa coefficients of the dry season and wet season of 0.90 and 0.845, respectively. There was a continuous decline in woodland (29.38%) and riparian vegetation (47.11%) and an increasing trend in shrub bush land (35.28%), grassland (43.47%), bare land (27.52%), and cultivated land (118.36 km^2) over the thirty-year period. Moreover, the results showed that bare land expanded from wet to drier months, while cultivated land and grazing land increased from dry to wet months. Based on the NDVI results, high to moderate vegetation was decreased by 21.47%, while sparse and non-vegetation expanded by 19.8% and 1.7%, respectively. Settlement and agricultural expansion, human-induced fire, firewood collection, gold mining, and charcoal production were the major proximate drivers that negatively affected park resources. Around KSNP, the local communities' livelihood depends on farming (crop and livestock production). This expansion of farming is the main driver of woodland depletion, which leads to increased resource competition and a challenge for the survival of wildlife. **Therefore**, urgent sustainable conservation of park biodiversity by encouraging community participation in conservation practices and preparing awareness creation programs should be mandatory.

1. Introduction

Land use land cover (LULC) change is a human-dominated modification of the terrestrial surface of the Earth (Ellis, 2006) and a significant environmental issue that affects the ecological processes encountered on a global scale (Klimanova et al., 2018; Sleeter et al., 2012). The assessment of LULC change is a study of environmental change that is more closely associated with the expansion of settlement following agriculture (Wang et al., 2018) and rapid urbanization and deforestation (Hassan et al., 2016). The consequences of LULC change include forest fragmentation and cover reduction, land degradation, biodiversity loss (Cheruto et al., 2016; Haregeweyn et al., 2015; Maitima et al., 2009), climate change (Agidew and Singh, 2017), and degraded habitat quality (Hassan et al., 2016). The changes also have significant environmental consequences for the fluctuation of local climate conditions, lowering ground water tables, and alteration in surface runoff (Bewket and Abebe, 2013; Lambin et al., 2003; Lambin and Geist, 2006). The change in LULC was more associated with the rural people livelihood that depends on mixed farming of crop production and livestock (Asmame and Abegaz, 2017). LULC change was caused by the expansion of agriculture through unplanned and inappropriate land management practices to meet the food demand of the local communities (Agidew and Singh, 2017). In many areas of developing countries, LULC changes caused by deforestation have increased the agricultural production of rural communities (Maitima et al., 2009) because their livelihood depends on natural resources (Mwavu and Witkowski, 2008). It also has important impacts on the functioning of socioeconomic and environmental systems, with tradeoffs for

* Corresponding author.
E-mail address: fitsetee21@gmail.com (F. Temesgen).

https://doi.org/10.1016/j.heliyon.2022.e12298
Received 18 May 2022; Received in revised form 14 October 2022; Accepted 5 December 2022

sustainability, food security, and biodiversity (Lesschen et al., 2005). LULC change via deforestation, urbanization, and intensified or extensified agriculture also created negative influences on the water cycle (Hisdal and Tallaksen, 2000).

LULC change is the combined temporal interaction of social, economic, institutional, and environmental factors (Hassan et al., 2016; Li et al., 2009; Lambin et al., 2001). These change factors influence the socioeconomic and living environments of the rural livelihood of many regions of Sub-Saharan Africa (Maitima et al., 2010). In this region, high poverty level, fuel production, expansion of settlement, and agriculture were prioritized as drivers for LULC change (Mekuyie et al., 2018; Kamwi et al., 2015; Kindu et al., 2015). Similarly, in semiarid areas of Ethiopia, the expansion of croplands and overharvesting of woodlands were major drivers of change (Zewdie and Csaplovics, 2016). The government-led resettlement program in Ethiopia was another core driver of LULC change because the program was undertaken without due consideration of natural resources and lacked a clear management plan for the sustainable utilization of resources (Yadeta et al., 2022; Mamude et al., 2021; Abera et al., 2020; Esa and Assen, 2017). Thus, the livelihood of resettled communities depends on the production of agricultural crops at the expense of woodland vegetation.

LULC change has increased the trend of biodiversity crises over the last four decades globally (Sharma et al., 2018; Butchart et al., 2010; Krauss et al., 2010). This global loss of biodiversity has great potential to interrupt relevant ecological processes and hinder ecosystem services that are essential for humans (Schmitz et al., 2014; Keesing et al., 2010). LULC change directly affects global biodiversity, which contributes to assessing recent regional and global climate change and future climate scenarios (Dwivedi et al., 2005; Fan et al., 2007). Currently, biodiversity is dominantly concentrated in protected areas (PAs) (Butsic et al., 2015; Coetzee et al., 2014; Geldmann et al., 2013). The resources in and around PAs are more critical in developing nations of the communities living adjacent to PAs because their livelihoods are often directly dependent on the resources (Hartter and Southworth, 2009). In most parts of the world, the activities of communities around PAs are expected to influence them negatively (Jones et al., 2018; Sala et al., 2000). LULC change around PAs has direct impacts on PA biodiversity and its ecological processes (Jones et al., 2009; Hansen and Defries, 2007). Over the last three decades, LULC change has been occurring rapidly in PAs and is projected to continue (DeFries et al., 2005; Beresford et al., 2018). Therefore, the evaluation and monitoring of LULC changes in and around PAs have become of paramount importance (Bailey et al., 2016).

The expansion of cultivated land has been largely at the expense of forests; globally, during the 1990s, there was an average loss of 16 million hectares of forests per year (FAO, 2011). Agricultural expansion has been reported to be the main driver of deforestation and lead to biodiversity loss (Haines, 2009; Lepers et al., 2005). A conversion of forest cover to other human-made land use, particularly to agriculture, was reported from PAs of the conterminous United States (Lu et al., 2018), Sagarmetha National Park, Nepal (Garrard et al., 2016), Semiarid, India (Duraisamy et al., 2018), and PAs forest, Mexico (Sancheza Reyes et al., 2017). The conversion of forests to agriculture has also become a major problem in East (Lambin et al., 2003) and South Africa (Bailey et al., 2016) due to rapid population growth and subsequent resource competition. In Ethiopia, anthropogenic activities are the most significant factors adversely altering natural resources (Marchant et al., 2018) and contributing detrimental impacts on the environment and livelihood of people (Tefera, 2011; Gebreslassie, 2014). Most of the studies of LULC change in Ethiopia have documented a considerable expansion of farmland at the expense of forest cover and other LULC (Lemenih et al., 2014). A study in the Eastern Tigray region revealed a strong decrease in forest and bushland in favor of arable and rangelands (Kassa et al., 2014). Similarly, in the Kafta Humera district (around the study site), agricultural land has largely expanded by shrinking the coverage of woodland (Alemu et al., 2015; Zewdie and Csaplovics, 2016). Extensive agricultural expansion as a cost of woodland and dense forest decline was also reported from Nechisar National Park (Fetene et al., 2015), Bale Mountain National Park (Nune et al., 2016), and Babile Elephant Sanctuary (Sintayehu and Kassaw, 2019).

Ethiopia is ecologically rich in biodiversity; however, the biological resources of plants and wild animals are gradually shrinking (Tefera, 2011). Forest disturbance and the rapid rate of deforestation in the country mainly occur due to poor resource management and government land policy (i.e., the national government needs to ensure rapid economic growth and poverty mitigation at the expense of natural resources (Othow et al., 2017). To combat these problems, Ethiopia has established 21 national parks, 2 wildlife sanctuaries, 6 wildlife reserves, 20 control hunting areas and priority forests, biosphere reserves, and community conservation areas since 1966 (Vreugdenhil et al., 2012). However, most of Ethiopia's PAs are increasingly degraded due to unsustainable natural resource management, habitat degradation due to livestock encroachment, illegal settlement, agricultural expansion, deforestation, border conflicts of local communities, uncertain land tenure, and very low public awareness of the importance of biodiversity and ecosystems (Young, 2012). Moreover, suitable wildlife habitats and their biological diversity are decreasing due to the destruction and fragmentation of natural habitats (Bekele and Yalden, 2013). However, the expansion of protected areas in Ethiopia is increasingly occurring, and the suitable wildlife habitats of almost all parks, including Kafta Sheraro National Park (KSNP), are collapsing gradually from time to time.

Land use land cover (LULC) change is key information for scholars who are working in land management studies (Karakas et al., 2015). Therefore, understanding the dynamics and driving forces of LULC changes at the local and global levels is fundamental in developing strategic planning and the analysis of land-related policies (Tekle and Hedlund, 2000). To announce each LULC change, remotely sensed (RS) and geographical information systems (GIS) are widely used data sources (Karakas et al., 2015; Karakus et al., 2014). Comparatively, the combination of RS data and field observations can accomplish LULC change detection more accurately than separately (Mucova et al., 2018) because satellite data analysis alone might miss the drivers of LULC change (Lambin and Meyfroidt, 2010). Human perception is significant for understanding LULC change patterns, driving forces, and consequences (Burgi et al., 2017; Grinblat et al., 2015). Moreover, LULC change analysis acceptance and accuracy were maximized when satellite image analysis was mixed with local residents' participation (Garrard et al., 2016; Nune et al., 2016; Kamwi et al., 2018). Therefore, the main objective of this study was to assess the extent of LULC change and the key drivers of change in Kafta Sheraro National Park (KSNP) between 1988 and 2018. The **specific objectives** were (1) to identify and delineate different LULC categories and to show the spatial and temporal trends of the main LULC change; (2) to assess the wet and dry season variations in NDVI and dry land forest vegetation cover change; and (3) to explore the causes/driving factors of LULC change by the socioeconomic conditions of the communities and their perceptions of LULC change and proximate drivers.

2. Materials and methods

2.1. Description of the study area

Kafta Sheraro National Park (KSNP) was designated a park in 2007 (Letter, No: 13/37/82/611) with an area of 2176.43 km^2. The park was formerly named the "Shire Wildlife Reserve" and was established in 1973 with an estimated area of 750 km^2 governed by the Tigray national regional state. Kafta Sheraro National Park (KSNP) is located in Kafta humera and Tahitay adiyabo weredas (districts) of the western and northwestern zones of the Tigray region 1356 km from Addis Ababa and 490 km from Mekelle city. The park is situated in northern Ethiopia between latitude 14°05′–14°27′N and longitude 36°42′–37°39′E. The park is bordered by Eritrea in the north and transverse by the Tekeze River (Figure 1). The elevation of the park varies from 539 to 1130 m

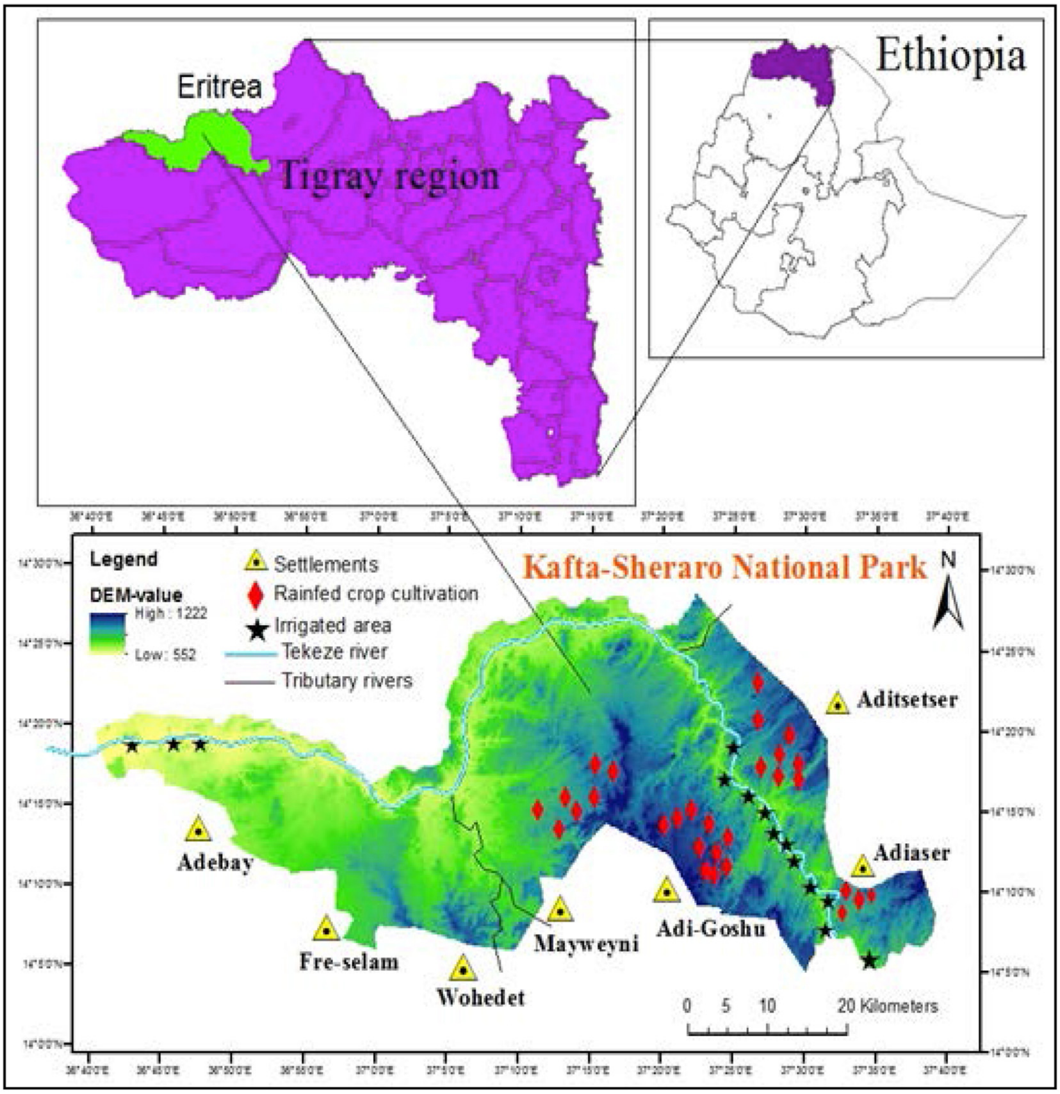

Figure 1. Location and elevation map of Kafta Sheraro National Park (KSNP) in the Tigray region.

above sea level (m.a.s.l.). The landforms of the areas are heterogeneous in nature and consist of a flat plain, undulating to rolling; some isolated hills and ridges, a chain of mountains, and valleys. The climate of the area is generally characterized by hot to warm semiarid and seasonal rainfall (Temesgen and Warkineh, 2020). The maximum monthly temperature is in April (43.7 °C), while the minimum monthly temperature is in December (19.2 °C) and January (19.1 °C). The mean monthly temperature ranges from 28.35 °C to 35.1 °C. The coolest temperature occurs in August, while the warmest temperature occurs from March to May. The rainfall pattern varies greatly with the months of the season. Short rains occur in June and September, and long rains occur during July (174 mm) and August (252 mm), whereas rare cases of rain in the remaining months appear (Figure 2).

The KSNP harbored more than 70 woody species, 46 trees, 18 shrubs, and 6 tree/shrubs. The most dominant and frequent tree species in the park are *Acacia mellifera*, *Combretum hartmannianum*, *Terminalia brownii*, *Balanites aegyptiaca*, *Dicrostachy scinerea*, *Acacia senegal*, *Acacia oerfota*, *Boswellia papyrifera*, *Ziziphus spina-christi*, and *Anogeissus leiocarpus* (Temesgen and Warkineh, 2020). The park is also home to large mammals such as African elephant, Roan antelope, Oribi, Spotted hyena, Greater kudu, warthog, Anubis baboon, Grivet monkey, crocodile, fish species and wintering migratory bird (Demoiselle crane) along the Tekeze River (Shoshani and Demeke, 2008). Agriculture is the main source of livelihood and economic activities of the studied settlers. The livelihood of the local communities of the districts Kafta humera and Tahitay adiyabo weredas (surrounding the park) is dominated by mixed farming of crop livestock production (Dejene et al., 2013).

2.2. Data collection and sources

2.2.1. Satellite image data

Landsat 5 thematic mapper (TM), Landsat 7 Enhanced thematic mapper plus (ETM^+), and Landsat 8 Operational land imager/Thermal infrared sensor (OLI/TIRS) multispectral satellite sensor data were used to detect LULC changes from 1988 to 2018 (Figure 3). The images were downloaded from Earth Explorer (http://earthexplorer.usgs.gov) and covered by the path/row (170/50) of the Worldwide Reference System. The images with high resolution and minimum or no cloud cover were selected from a number of images for each period to minimize errors or confusion for classification. A total of 26 images for the dry and wet seasons, 5 for LULC change detection, and 21 for normalized difference vegetation index (NDVI) analysis were downloaded. The dry season period of the area was defined from November to May, and the wet season was defined from June to October. However, the images were taken for the wet season between September and October and for the dry season between March and April. These months were preferred for all

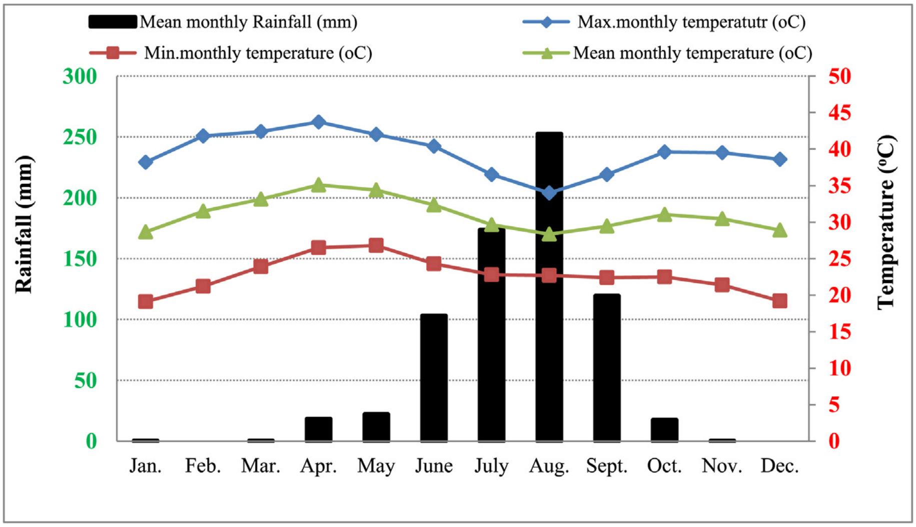

Figure 2. Maximum, mean, and minimum monthly temperature (°C) and mean monthly rainfall (mm. month^{-1}) of Humera and Sheraro Districts Meteorological Center (1996–2016); Source = Ethiopian National Meteorology Agency (ENMA, 2018).

satellite image sensors because they were found to have no or minimum cloud cover and water vapor. A detailed explanation of each satellite sensor is described in Table 1 for LULC change classification and for NDVI analysis in Table 2.

2.2.2. Field observation data

Field visits were carried out from December 2018 to April 2018 for the dry season and from mid-June 2018 to the beginning of November 2018 for the wet season to identify major LULC types and to take field training points that are changed seasonally in the KSNP. Table 3 shows LULC change identified in the field in each season and cross-checked through interviews of local farmers' focus group discussions (FGDs) with farmland inside and around the park. Accordingly, the local farmers interviewed that the plowing and sowing time of rain fed crops starts in June and that the crops are harvested from mid-November to December. After the rain fed crops are harvested, they could leave the land bare until the next sowing year (June) or be left totally free and shifted to a new area. Similarly, the grasses covered in the wet season appeared bare until the next rainy season (Table 3).

Fieldwork is mainly focused on observing and capturing the various LULC types using a digital camera, and each sampling location was recorded via the geographical positioning system (GPS) of handheld

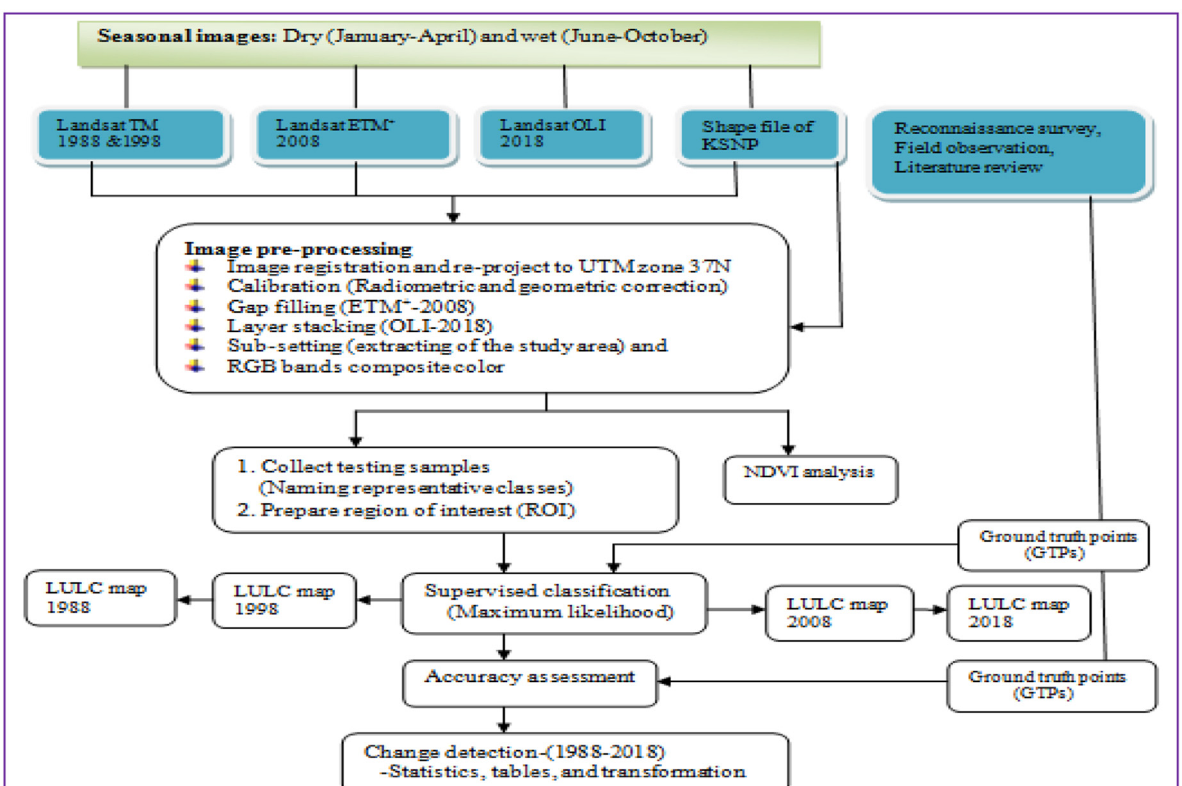

Figure 3. Flow diagram summary of steps and data utilized in image analysis.

Table 1. Data type and detailed description of satellite images used in LULC change analysis.

Satellite	Sensor type	Path/Row	Acquisition date	Spatial Resolution(m)	Bands (B) used for spectral signature	Bands wave length (μm)
Landsat5	TM	170/50	23-10-1988	30	B1, B2, B3, B4, B5, B7	0.48–2.20
Landsat5	TM	170/50	19-10-1998	30	B1, B2, B3, B4, B5, B7	0.48–2.20
Landsat7	ETM^+	170/50	06-10-2008	30	B1, B2, B3, B4, B5, B7	0.48–2.22
Landsat8	OLI/TIRS	170/50	10-10-2018	30	B2, B3, B4, B5, B6, B7	0.45–2.29
			16-03-2018			

Note: TM = thematic mapper, ETM^+ = enhanced thematic mapper plus, OLI = operational land imager, TIRS = thermal infrared sensor, B = band, μm = micrometer, m = meter and calendar order (day-month-year).

Garmin GPS-60. To emphasize, the classification was more accurate; more than 100 ground truths (latitude and longitude records) were collected from each LULC type of the 2018 image, and a total of 700 points were collected for seven classes. The accuracy assessment was basically good for the Landsat-8 (OLI) of the 2018 satellite image because the points directly show the recent feature of LULC categories. The ground control points were divided into two groups: one group for selecting training sites for classification and the second group for the accuracy assessment.

2.2.3. Socioeconomic survey

Sampling design: The drivers of LULC change in the study were collected from three basic sources: (1) household questionnaires, (2) focus group discussions, and (3) key informant interviews. As the park is located in two weredas (districts) of Kafta humera and Tahitay adiyabo, seven Kebeles (the smallest governmental administrative units of Ethiopia) were purposively selected from the total, based on proximity to the park and their livelihood directly dependent on the resources of KSNP and its surrounding area. A systematic sampling method was used to select the representative sample respondents for the household interviews from individual kebeles, whereas the purposive sampling technique was used for focus group discussion and key informant interviews. The sample size of households was calculated using equ. (1) Sampling technique (Cochran, 1977).

Table 2. Detailed description of satellite images used for normalized difference vegetation index (NDVI) analysis.

Satellite ID	Sensor type	Path/ Row	Acquisition date	Spatial Resolution(m)	Sources
Landsat 5	TM	170/50	13-03-1988	30	USGS
Landsat 7	ETM^+	170/50	20-10-2007	30	USGS
		170/50	26-03-2007	30	
		170/50	06-10-2008	30	
		170/50	28-03-2008	30	
		170/50	09-10-2009	30	
		170/50	16-04-2009	30	
		170/50	12-10-2010	30	
		170/50	18-03-2010	30	
		170/50	15-10-2011	30	
		170/50	21-03-2011	30	
		170/50	01-10-2012	30	
		170/50	08-04-2012	30	
Landsat 8	OLI/TIRS	170/50	26-09-2013	30	USGS
		170/50	28-03-2013	30	
		170/50	29-09-2014	30	
		170/50	21-03-2014	30	
		170/50	16-09-2015	30	
		170/50	08-03-2015	30	
		170/50	20-10-2016	30	
		170/50	26-03-2016	30	

Note: TM = thematic mapper, ETM^+ = enhanced thematic mapper plus, OLI = operational land imager, TIRS = thermal infrared sensor, USGS = United States Geological Survey, calendar order (day-month-year).

$$no = \frac{t^2 pq}{e^2};\ n = \frac{no}{1 + \frac{(no-1)}{N}} \tag{1}$$

where, no = assumed simple random sample size of households (384); p = estimated proportion of the population to be included in the sample (i.e., 50%); q = 1 − p; t = uncertainty (number of standard errors) in the number of people depending on park resources of ±5% (at the 95% confidence interval level, Z value = 1.96); e = the margin of error (0.05); n = sample size, and N = the total number of household heads (i.e., 5458). Using Eq. (1), the result of the sample size was 359; however, to compensate and cover the non-response of households, the sample size was increased by 10% (36). Therefore, the total sample size of the selected households in this study was 395 (Table 4).

For questionnaire distribution, households were systematically selected from each kebele. Thus, the first household selection started randomly from the settled households, and then the next households were selected systematically at every 9th interval in each kebele using the formula below until the given sample size was reached. Therefore, the size of the interval (k) for selection was calculated by k = N/n, where k = the size of the interval for selection; N = total population (households); and n = the number of samples required for the study (Mota et al., 2019).

Household survey: The questionnaires had both open and closed-ended questions to gather information about the perceptions of the local communities on LULC changes and the drivers of change in KSNP from November 2018 to June 2019. The questionnaires covered 395 households from seven Kebeles (Table 4), and individual household responses took 50–70 min. The targeted populations for semi structured interviews were parks near communities (villagers) having direct interaction with KSNP, irrigation farm holders, and livestock owners. The questionnaires were designed to gather general household characteristics, forest coverage trends, perception of the local people on LULC change, and the drivers of change (Appendix-1).

Focus group discussions (FGDs): The investigator will collect data by gathering a group of participants together to discuss the relevant issue of the study. The FGDs were performed within seven Kebeles in the study area by involving elderly people who were older than 60 years and lived in the area for more than 28 years. The elders were consulted for the age and history of the land use type and the main drivers of LULC change of KSNP using open-ended questions. This has helped us to be aware of the ongoing LULC change (past and present drivers of LULC change) in the study area.

Key informant interviews (KII): The main objective of the key informant interviews was to collect detailed information from a wide range of people who selected specific groups who had first-hand information about the

Table 3. Some of the LULC classes change seasonally or remain the same, and the field points are set for the two seasons (wet and dry).

Land use land cover classes	Wet season	Dry season
1. Rain fed crops	Cultivation	Bare land
2. Grazing/grass cover	Grass land	Bare land
3. Irrigated land	Cultivation	Cultivation
4. Streams & main tributary rivers	Water body	Bare land
5. Main road	Bare land	Bare land
6. Sandy and small gravel area	Bare land	Bare land

Table 4. Total selected sample household heads from seven Kebeles of Kafta humera and Tahitay Adiyabo districts (Source: survey 2018/19).

Wereda (district)	Selected Kebeles	Total heads of household	Sample size has taken from each kebele		
			Male	Female	Total
Kafta-humera	Adebay	2976	88	36	124
	Freselam	291	25	9	34
	Wuhedet	262	21	7	28
	Mayweyni	265	22	8	30
	Adigoshu	671	55	17	72
Tahitay adiyabo	Adiaser	324	28	9	37
	Aditsetser	669	51	19	70
Total		5458	293	102	395

ongoing problems that happened in KSNP by the communities. The qualitative data collection from key informants was via direct individual interviews and focus group discussions. Thus, the researcher conducted three key informant interviews: (1) community administrators and professional experts (i.e., crop and livestock production, forest and wildlife conservation, soil and water conservation) of the study districts; (2) religious leaders in the districts; and (3) management, experts, and scouts of KSNP.

The questionnaire for focus groups (elderly people) and key informant interviews were arranged for qualitative data collection by preparing the outlined script and a list of open-ended questions from specific topics of the study objectives (i.e., forest cover trend, past and present LULC, causes of LULC change, and community attitude to LULC change). The questions prepared by the investigator for elderly people were short, clear, and phrased in their local language (i.e., Tigrigna), while for expert and professional informants; the questionnaires were broad and more formally phrased. Moreover, the selected groups engaged in detailed discussions, elaborations, and conversations on the issues raised (questionnaires). Finally, the investigator recorded the interview response both by note taking and audio recording.

2.3. Data analysis

2.3.1. Preprocessing of images

Before LULC classification and detection of changes, preprocessing of satellite images is an imperative process to develop an inline association between biophysical phenomena on the ground and acquired data (Coppin et al., 2004). Before any activities, Landsat images (TM 1988 and 1998, ETM$^+$ 2008 and OLI 2018 imageries) were geometrically rectified (geocoded) to the World Geodetic System 1984 (WGS 84) and set a projection to Universal Traverse Mercator (UTM) zone 37 N specific to Ethiopia. Geometric and radiometric (reflectance) calibration: During image acquisition, satellite images have different types of distortions/noise, which reduces the quality of the image. The calibration of Landsat imagery was performed based on the known solar geometry and on the gain and bias values provided by the Landsat metadata (Hilker et al., 2012). For better performance of the Landsat time series of LULC change analysis, consistent image sets of geometric and radiometric corrections are the two significant activities (Rani et al., 2017; Hansen and Loveland, 2012). For the present study, geometric and radiometric (reflectance) corrections were carried out to decrease negative atmospheric effects or correct for changes that occurred in scene illumination, atmospheric solar conditions, and viewing geometry, as applied by Chander et al. (2009). Likewise, images with clouds and cloud shadows were removed using a cloud mask (*fmask function*) with the ArcMap10.5 tool. Subsequent calibration activities, such as gap filling, layer stacking, and sub setting of bands, were undertaken.

2.3.1.1. Band color combination. This activity refines image interpretability by increasing differentiability among objects of the image for classification. According to Mohy et al. (2016), visual interpretation of images is an important step toward understanding the area of specific study and preparing for field surveys. Chavez et al. (1982) developed a quantitative statistical technique called the optimum index factor (OIF) that improves image visualization and selection of Landsat image band ratio color combination (Eq. (2)). The optimum index factor (OIF) was based on the variance (i.e., standard deviation) and the correlation among the different band ratios. The authors reported that the ratio combination with the largest OIF value that contained the most information content and the least amount of decomposition (lowest correlation coefficients) was selected for the optimum color composite.

$$\mathrm{OIF} = \frac{\sum_{i=1}^{3} SDi}{\sum_{j=1}^{3} |CCj|} \tag{2}$$

where, Sdi = standard deviation for ratio i; |CCj| = absolute value of the correlation coefficient between any of the three band color ratios.

In this study, for better visualization of different objects in the images, we created a color combination by taking band 7 for infrared (2.064–2.345 μm), 4 for near-infrared (1.547–1.749 μm), and 1 for blue (0.772–0.898 μm), which were chosen for TM 1988, 1998 and ETM$^+$ 2008. For OLI 2018, band 7 for infrared (2.107–2.294 μm), band 5 for near-infrared (0.851–0.879 μm), and band 4 for red (0.636–0.673 μm) were chosen. The preprocessing activities were performed using ENVI 5.3 software.

2.3.2. Land use/cover class classification

The images were classified using the supervised classification algorithms under ENVI 5.3 because we are familiar with the study landscape. This classification method may be preferable for LULC change detection if prior information about the landscape is gained through personal knowledge of the study area (Rogan and Chen, 2004). The individual LULC class signatures of polygons (training areas) were marked based on field observations, household knowledge, and color combinations of bands (image visual interpretation). Then, the image data set in the LULC class is placed via the maximum likelihood classifier (MLC). Even though there are different classifiers, the MLC algorithm was better performed using all the spectral bands fit to vegetation (Abyot et al., 2014; Rawat et al., 2013; Manandhar et al., 2009). This technique also has a greater probability of weighting minority classes that can be swamped by the large class during training samples taken from images. The minority classes in the image have the opportunity to be included in their respective spectral classes (reduce uncategorized pixels) from entering into another class (Othow et al., 2017). Accordingly, seven major LULC classes were recognized in KSNP, and their description was based on the author's prior knowledge of the study site and detailed field observations (Table 5).

2.3.3. Accuracy assessment

Accuracy assessment is useful to assess the quality of the data collected in the field and the classified images. This technique determines the sources of error encountered during the classification of satellite images (Congalton and Green, 2009). Accuracy assessment determines how accurate the ground truth data region of interest agreed with classified images of the remotely sensed data in which precision testing was conducted using the Kappa index (Keshtkar et al., 2017; Smits et al., 1999). We compare the accuracy assessment of 1988, 1998, and 2008 using ground sample points taken from Google Earth maps, long-lived resident interviews, and previously published research reports. However, for the dry and wet seasons of the 2018 satellite image classification and accuracy assessment analysis, 100 points from each of the 7 classes (total of 700 points) of ground truth data in the form of reference points were collected using a geographic positioning system (GPS). Generally, the accuracy assessment was expressed using four parameters: user's accuracy, producer's accuracy, overall accuracy, and kappa coefficient, which were derived from the error (confusion) matrix following Eqs. (3), (4), (5), and (6) (Lillesand et al., 2008; Congalton and Green, 2009; Liu et al., 2007; Lung and Schaab, 2009).

Table 5. Land use/cover categories and their explanations in Kafta Sheraro National Park (KSNP).

LULC type	Description
Woodlands	Large and medium trees which have medium canopy cover arise from lower range of grasses and herbs.
Shrub-bush lands	Dominantly covered by short height shrub/bush structure of plants and arise from mixed lower coverage of grasses and herbs.
Riparian forests	Dense canopy cover vegetation of the park along Tekeze River and its tributary rivers valley having vertical stratification and dominated by tall trees or wood lands.
Grasslands	Plains, rough ground and relatively hilly areas cover by different predominantly grass species mixed with herbs and natural pasture for animals.
Agricultural land	Both rain fed crops and irrigated vegetable and fruit crops like banana and mango plantation. Areas of store house and farmhouses are also under agricultural land.
Water bodies	Water courses of Tekeze river, permanent and seasonal tributary rivers, and streams
Bare land	Areas including no vegetation cover, gravel and asphalt roads, degraded lands, bare ground and gold excavation areas, mixed sand and small gravel which are found in Tekeze River sides and its tributary rivers.

$$\text{User's accuracy (UA)} = \frac{\text{Number of correctly classified pixels in each catagory}}{\text{Total number of reference pixels in that catagory (row total)}} \times 100\% \tag{3}$$

$$\text{Producer's accuracy (PA)} = \frac{\text{Number of correctly classified pixels in each catagory}}{\text{Total number of reference pixels in that catagory (column total)}} \times 100\% \tag{4}$$

$$\text{Overall accuracy (OA)} = \frac{\text{Total number of correctly classified pixels (Diagonal)}}{\text{Total number of reference pixels}} \times 100\% \tag{5}$$

$$Kappa\ coefficient(Kc) = \frac{N\overset{m}{\Sigma}Dij - \overset{m}{\Sigma}Ri.Cj}{N^2 - \sum Ri.Cj}\,_{i,j=1} \tag{6}$$

where, N = total number of pixels, m = number of classes, ΣDij = total diagonal elements of an error matrix (the sum of correctly classified pixels in all images), Ri = total number of pixels in row i, and Cj = total number of pixels in column j. The value of Kc ranges between +1 and −1.

2.3.4. Land use land cover (LULC) change

The magnitude of change is a degree of expansion (+) or reduction (−) in the LULC size of the classes. The percent rate of LULC change was computed by Eq. (7) (Duraisamy et al., 2018; Bekele et al., 2019; Asmame and Abegaz, 2017; Esa and Assen, 2017).

$$\text{Change rate (\%)} = \frac{\text{Area of final year} - \text{area of initial year}}{\text{Area of initial year}} \times 100 \tag{7}$$

The annual rate of change per year was calculated using Eqs. (8) and (9) (Alawamy et al., 2020).

$$\text{Annual rate of change } (\text{km}^2/\text{year}) = \frac{\text{Area of final year} - \text{area of initial year}}{\text{Time interval b/n initial \& final years}} \tag{8}$$

$$\text{Annual rate of change (\%)} = \frac{\text{Area of final year} - \text{area of initial year}}{(\text{Time interval b/n initial \& final years}) \times (\text{Area of initial year})} \times 100 \tag{9}$$

2.3.5. Normalized difference vegetation index (NDVI) analysis

The normalized difference vegetation index (NDVI) is used to distinguish the forest cover status, state of degradation, and extent of loss (Meneses-Tovar, 2011). Thus, NDVI information is relevant in the study area because the local community influence on forest cover is relatively high. Landsat images from 1988 and 2018 were utilized to extract NDVI values of vegetation cover change classification as nonvegetation, sparse vegetation, and high to moderate density vegetation (Figure 8 and Table 11). The NDVI value ranges between −1 and +1. As the value increases toward +1 or increasing positive NDVI values indicate dense vegetation (vegetated plant canopy), and values close to zero or decreasing negative values (−1) indicate nonvegetation surfaces such as water and bare ground (Schnur et al., 2010). NDVI has a high positive value in vegetated agricultural cover crops (Meneses-Tovar, 2011). NDVI is calculated based on the difference in the ratio of red (R) and near infrared (NIR) reflectance using Eqs. (10) and (11) (Naif et al., 2020; Bilgili et al., 2014).

$$\text{Landsat}-8, \text{NDVI} = \frac{\text{Near\_ infrared (band 5)} - \text{Red (band 4)}}{\text{Near\_ infrared (band 5)} + \text{Red (band 4)}} \tag{10}$$

$$\text{Landsat}-5,7\ \text{NDVI} = \frac{\text{Near\_ infrared (band 4)} - \text{Red (band 3)}}{\text{Near\_ infrared (band 4)} + \text{Red (band 3)}} \tag{11}$$

Note: In this analysis, the index was computed based on the difference in red band 4 (0.64–0.67 μm) reflectance and NIR band 5 (0.85–0.88 μm) reflectance of Landsat-8 OLI of both dry (March 2018) and wet season (October 2018) satellite images. In addition, for the TM and ETM$^+$ sensors, the red band was 3 (0.63–0.69 μm), and the NIR band was 4 (0.77–0.9 μm).

The study site is located in a semiarid region, where climate variables are limiting factors for vegetation cover determination. From the climate variables, precipitation has a direct relation with the spatial and temporal changes in the NDVI. Due to the absence (discontinuous) of remotely sensed satellite images between 1996 and 2006, the NDVI relation with climate variable analysis was conducted between 2007 and 2016. In these periods, continuous satellite image data were directly matched with the recorded precipitation and temperature of the same years and seasons. Thus, the statistical relationship between the NDVI response and precipitation and/or temperature separately was examined through a simple linear regression model for one decade of data as applied with Eq (12).

$$\text{NDVI} = a \pm b^{*}\text{rainfall or temperature} + \varepsilon \tag{12}$$

where, 'NDVI' = dependent factor; rainfall or temperature = independent factor, a = intercept, b = partial slope coefficient for variable rainfall or temperature, and ε = random error. The seasonal mean NDVI, annual seasonal rainfall, and seasonal mean temperature were analyzed for the period from 2007 to 2016. The significance of the mean NDVI change was evaluated at the 95% confidence level ($p < 0.05$).

2.3.6. Socioeconomic and associated statistical analysis

The data collected from sampled households were quantitatively analyzed, whereas data from focus group discussions (FGDs) and key informant interviews were analyzed qualitatively. Descriptive statistics, such as the mean and percentage, were used to describe the socioeconomic variables of the households and summarize their responses using tables and figures. Statistically, the interviewees' awareness of the drivers of LULC change response between selected socioeconomic variables was analyzed by Pearson's chi-square (nonparametric test). The main drivers of LULC change obtained from the household surveys were summarized by the ranking method. In this method, the index was calculated as a ranking ratio with the principle of weighted average adopted by Musa et al. (2006), as described in equ (13).

$$\text{Index} = \frac{R_n{}^{*}C_1 + R_{n-1}{}^{*}C_2 + \ldots + R_1{}^{*}C_n}{\Sigma R_n{}^{*}C_1 + R_{n-1}{}^{*}C_2 + \ldots + R_1{}^{*}C_n} \tag{13}$$

where, R_n = the value given for the least ranked level by respondents (in this study, the least rank is 4th, then $R_n = 4$, $R_{n-1} = 3$, & $R_1 = 1$); C_1 = the counts of the 1st ranked, C_2 = the counts of the 2nd ranked... & C_n = the counts of the least ranked level (in this study, C_n = the count of the 4th rank).

On the other hand, the local people's awareness status of LULC change drivers of KSNP, which is determined by the socioeconomic descriptive variable difference of the sampled households, was tested by logistic regression analysis. Logistic regression analysis is the interaction among the driver data and the LULC change category. Lesschen et al. (2005) stated that logistic regression is useful for discrete dependent variables that have a binary (bivariate) outcome and investigates the association of dependent (response) variables with independent variables. Therefore, the interlinked mathematical formula is summarized in equ (14).

$$\text{Logit}\ (Y) = \alpha + \beta_1X_1 + \beta_2X_2 + \beta_3X_3 + \ldots\ \ldots\ \ldots + \beta_kX_k \tag{14}$$

where, Y = the dependent (response) variable, α = the intercept, $\beta_1 \ldots \beta_k$ = the regression coefficients of explanatory variables, and $X_1 \ldots X_{k\ (7)}$ = the independent (explanatory) variables.

In the present study, the dependent variable was the difference in household awareness of the drivers of LULC changes, while the independent variables consisted of the descriptive information of the sampled households. Hence, there were seven determinant socioeconomic variables used in the analysis: age categories, gender, household size, education level, settlement duration, agricultural land size, and distance from settlement to the KSNP border. Thus, this analysis evaluated the impact probability of the independent variables on the dependent variables. Additionally, the correlations between the trends of different LULC change types were computed, and a statistically significant association was identified at $p < 0.05$. All the above-listed statistical tests (i.e., Pearson's chi-square (X^2), regression and correlation) were performed

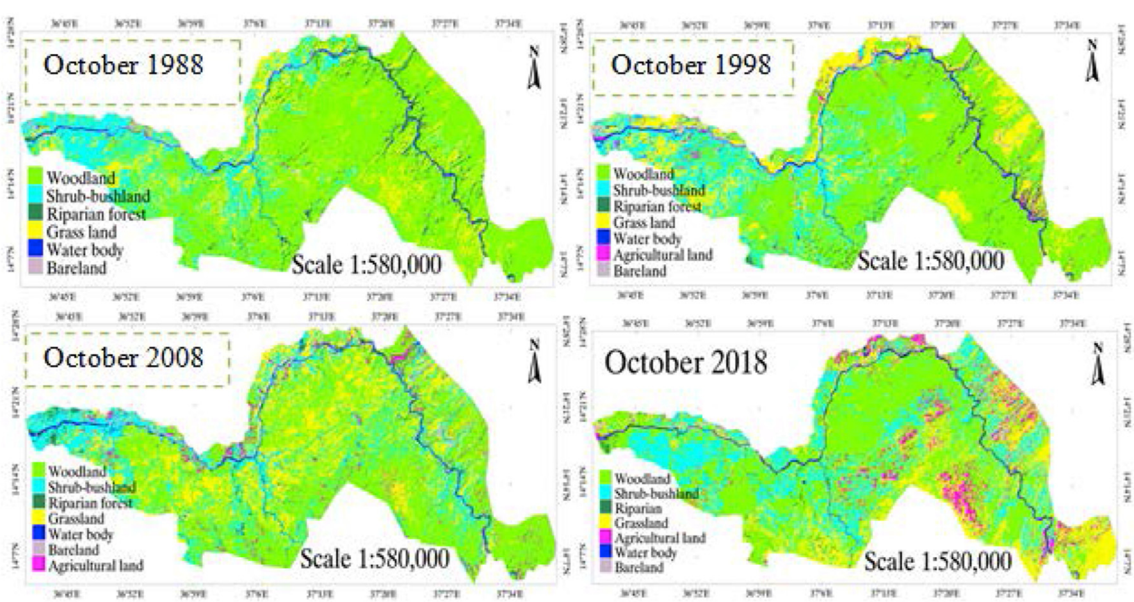

Figure 4. Wet season land use/land cover change class map derived from October 23, 1988, October 19, 1998, October 06, 2008, and October 16, 2018, Landsat images.

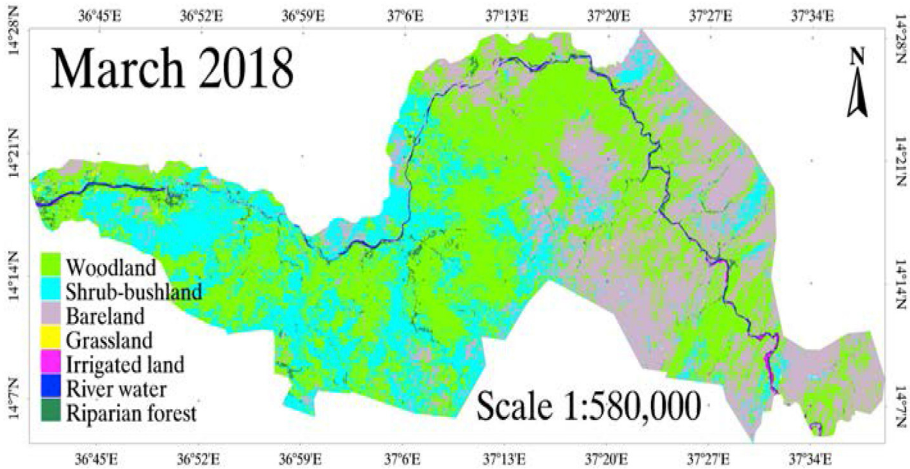

Figure 5. Dry season land use/land cover class map derived from March 16, 2018, Landsat image.

Table 6. Accuracy assessment (error matrix) for 1988, 1998, and 2008 Landsat images.

Land use land cover classes	1988		1998		2008	
	UA (%)	PA (%)	UA (%)	PA (%)	UA (%)	PA (%)
Woodland	90.46	87.15	93.79	94.15	88.69	66.54
Shrub-bushland	77.65	82.20	84.20	92.39	75.54	86.64
Riparian forest	93.73	85.40	64.06	86.77	76.81	91.33
Grassland	77.57	96.35	96.92	88.59	75.47	94.65
Agricultural land	–	–	64.78	73.03	68.03	60.58
Water body	100.00	97.84	97.06	88.55	99.30	85.94
Bareland	97.71	95.09	87.09	95.87	95.31	96.64
Overall accuracy (OA)	88.6%		88%		82.26%	
Kappa coefficient (Kc)	0.85		0.84		0.79	

UA = user accuracy, PA = producer accuracy.

using R-statistical Package (R-Core Team, 2019) and IBM SPSS statistics (IBM Corp, 2019).

2.3.7. Ethics approval and research site permission

The study ethics were reviewed and approved by the College of Natural & Computational Science, Research Department Graduate Committee (DGC, 2018) and Ethiopian Wildlife Conservation Authority Research Ethics Review Committee. Prior to the field visit and data collection, a permission letter was obtained from the Ethiopian wildlife conservation authority for the selected study site of Kafta Sheraro National Park (KSNP). Before distributing the questionnaire, the objective of the study was briefly explained to participants, and verbal consent was collected. The questionnaire excluded personal identifiers (privacy) such as the names of interviewees.

3. Results and discussion

3.1. Land cover classification map and seasonal variation of accuracy assessment

The LULC spatial distributions of Kafta Sheraro National Park (KSNP) were classified well in both the wet season from 1988 to 2018 (Figure 4) and the dry season in 2018 (Figure 5). The overall accuracies (OA) during 1988, 1998, and 2008 were 88.6%, 88%, and 82.26%, respectively, while the Kappa coefficients (Kc) were 0.85, 0.84, and 0.79, respectively (Table 6). The wet and dry season classification accuracy assessment of KSNP is considered reliable and acceptable agreement for the classified image of 2018. Based on the ground truth recorded data of 2018, the overall accuracies (OA) for images of wet and dry seasons were 86.9% and 91.96% with Kappa coefficients (Kc) of 0.845 and 0.90, respectively (Tables 7 and 8). The wet season OA and Kc of the study were higher than those of the Central Rift Valley of Ethiopia (Mesfin et al., 2020), protected and communal areas of Namibia (Kamwi et al., 2018), and Quirimbas National Park, Mozambique (Mucova et al., 2018). Similarly, the dry seasons of OA and Kc are also higher than the Bale Mountain National Park, Ethiopia (Nune et al., 2016), Maputaland-Pondoland-Albany Biodiversity hotspot (Bailey et al., 2016), and Tarangire and Katavi National Parks (Mtui et al., 2017).

Table 7. Wet season confusion matrix for the 2018 OLI classified image.

Classified data	Ground truth data								
	Wood land	Shrub bushland	Riparian forest	Grass land	Agricultural land	Water body	Bare land	Total	UA (%)
Woodland	129	0	7	0	1	0	0	137	88.97
Shrub-bushland	6	92	0	6	0	0	0	104	88.46
Riparian forest	0	0	128	0	0	0	0	128	96.80
Grass land	0	22	0	146	1	0	14	183	73.00
Agricultural land	0	0	0	1	88	0	0	89	98.88
Water body	1	0	0	0	0	74	0	75	98.67
Bareland	0	5	0	18	0	0	88	111	79.28
Total	136	119	135	171	90	74	102	827	-
PA (%)	88.36	77.31	89.63	82.49	93.62	98.67	85.44	-	-
Over all accuracy	86.9%								
Kappa coefficient	0.845								

Note: classes are shown by the number of classified pixels, UA = user accuracy, PA = producer accuracy.

Table 8. Dry season confusion matrix result for the 2018 OLI classified image.

Classified data	Ground truth data								
	Wood land	Shrub bushland	Riparian forest	Grass land	Irrigated land	River water	Bare land	Total	UA (%)
Woodland	117	28	2	1	0	0	6	154	76.47
Shrub-bushland	1	79	0	5	0	0	0	85	92.94
Riparian forest	0	2	53	0	0	0	0	55	96.36
Grassland	0	0	0	46	0	0	0	46	100
Irrigated land	0	0	0	0	0	0	0	98	100
River water	0	0	0	0	98	0	0	109	100
Bare land	2	0	0	0	0	109	66	68	97.06
Total	120	109	55	52	98	109	72	615	–
PA (%)	97.50	72.48	96.36	72.73	100	100	91.67	–	–
Over all accuracy	91.96%								
Kappa coefficient	0.90								

Note: classes are shown by the number of classified pixels, UA = user accuracy, PA = producer accuracy.

Table 9. Area extent of land use/land cover types in 1988, 1998, 2008, and 2018.

Land use land cover classes	1988		1998		2008		2018	
	km^2	%	km^2	%	km^2	%	km^2	%
Woodland	1,251.88	57.98	1,132.08	52.44	1,007.32	46.66	884.03	40.95
Shrub-bushland	374.91	17.36	402.36	18.64	436.82	20.23	507.18	23.49
Riparian forest	83.77	3.88	60.92	2.82	52.48	2.41	44.31	2.05
Grassland	371.03	17.18	417.52	19.34	496.35	22.99	532.34	24.66
Agricultural land[a]	0.00	0.00	64.79	3.00	95.57	4.45	118.35	5.48
Water body	48.30	2.24	49.22	2.28	34.59	1.60	35.02	1.62
Bareland	29.13	1.35	32.09	1.48	35.85	1.66	37.75	1.75
Total	2,159	100	2,159	100	2159	100	2159	100

[a] Cultivation area was absent in 1988, but crop cultivation clearly started in 1993.

Table 10. Magnitude and annual rate of change in different LULC categories of KSNP from 1988-2018*.

Land use land cover classes	1988–1998		1998–2008		2008–2018		Change between 1988-2018		Annual rateof change/year 1988–2018	
	km^2	%	km^2	%	km^2	%	(km^2)	%	(km^2)	(%)
Woodland	−119.81	−9.57	−124.8	−11.0	−123.3	−12.2	−367.85	−29.38	−12.3	−0.98
Shrub-bushland	27.45	7.32	34.46	8.56	70.36	16.1	132.27	35.28	4.41	1.17
Riparian forest	−22.85	−27.3	−8.78	−14.4	−7.83	−15.0	−39.46	−47.11	−1.32	−1.57
Grassland	46.49	12.53	78.82	18.88	35.99	7.25	161.31	43.47	5.38	1.45
Agricultural land	64.80	–	30.78	47.5	22.78	23.8	118.36	–	3.94	–
Water body	0.92	1.89	−14.63	−29.7	0.42	1.23	−13.29	−27.51	−0.44	−0.92
Bareland	2.94	10.08	3.78	11.8	1.30	3.61	8.02	27.52	0.27	0.92

*Negative sign (−) indicates that the land use/land cover class was decreasing in the entire time span.

The user's accuracies (UA) and producer's accuracies (PA) of the wet season woodland, riparian forest, agriculture, and water body were greater than 88% reasonably classified for the tested year (Table 7). Dry season riparian forest, irrigated land, river water, and bare land were relatively well classified, above 91% for all tested maps (Table 8). Comparatively, the dry season accuracy in 2018 was quantified to be higher than that in the wet season, and these results are in agreement with a study in tropical semiarid areas (Msigwa et al., 2019). These authors tested and approved that wet and dry seasonal accuracy exhibited an increasing trend from wet to drier seasons. In our study, the low classification accuracy or higher confusion error of the wet season grassland and woodland cover in 2018 was mostly caused by confusion with other related land cover classes. For example, in the wet season, grass is often confused with cultivation, and woodland is confused with shrub-bush land due to the limited spatial resolution and image quality (Msigwa et al., 2019) also observed that wet season grassland had low classification accuracy. As reported by Duraisamy et al. (2018), during the wet season, there was a high vegetative cover of crops and natural vegetation, which creates confusion or makes it difficult to differentiate among them. Furthermore, a study in Burkina Faso also revealed the highest classification accuracy in the dry season and the lowest classification accuracy in the wet season (Liu et al., 2007).

3.2. Trends of land use/land cover change during the period 1988–2018

Kafta Sheraro National Park (KSNP) experienced extensive LULC change due to increased settlement coupled with the expansion of farming activities from 1988 to 2018. However, woodland area coverage during 1988 was the largest; a continuous decline was observed in the three consecutive decades of the study period. The highest decline was observed from 1998 to 2008 by 11.0% (124.8 km^2), while the lowest decline was 9.57% (119.81 km^2) between 1988 and 1998. In thirty years (1988–2018), woodland decreased by 29.38% (367.85 km^2) at an average rate of 12.3 km^2 (0.98%) per year (Tables 9 and 10). The riparian forest declined consecutively from 1988 to 1998 and 1998 to 2008 by 27.3 km^2 (22.85%) and 14.4 km^2 (8.78%), respectively. However, in the 3rd period (2008–2018), the forest slightly declined by 7.83 km^2 (15%). In the three decade study, this class decreased by 39.46 km^2 (47.11%) at an annual rate of 1.32 km^2 (1.57%) per year (Tables 9 and 10). Because these periods took place, widespread expansion of dry season irrigated land and wet season rain fed crops occurred. The increase in settlement around the park, agricultural expansion, and firewood collection had a great impact on the destruction of woodland cover. The depletion of the Tekeze riverside riparian forest was due to extensive irrigated crop cultivation undertaken since 1993. In contrast, the dry season of bare land, agricultural land, grassland, and shrub bush land was highly expanded throughout the study period (1988–2018). Similar findings were reported from the Babile elephant sanctuary (1977–2017) study, in which woodland and riparian forests decreased, whereas agricultural land and bare land continuously increased (Sintayehu and Kassaw, 2019). In contrast to the present finding, the authors found a reduction in shrub bush land, as this class of land cover was the second next to woodland in their study periods. Birhane et al. (2018) also supported that shrub land was the dominant land cover from 1985 to 2015 in Hugumburda National forest priority areas that declined. Farmland expansion at the expense of woodland decline was also stated in Bale Mountain National Park (Muhammed and Elias, 2021; Solomon et al., 2014). Shrub land, grass (grazing land), settlement, cultivation, and bare land increased as the cost of forestland declined (Asmame and Abegaz, 2017). More studies from the central Rift Valley of dry land in Ethiopia revealed that areas of cropland doubled, and grass/grazing land and bare land increased as extensive woodland was destroyed between 1986 and 2016 (Mesfin et al., 2020; Bekele et al., 2019; Garedew et al., 2009). Moreover, in advance of cultivated land, a remarkable increasing trend was shown mainly at the expense of forest cover (Berihun et al., 2019; Bewket and Abebe, 2013). Abera et al. (2020) reported that woodland and dense forest decreased by 34.6% and 59.9%, respectively, while cultivation expanded by 15.16 km^2/year. Therefore, including the current study in KSNP, all the listed case studies in Ethiopia showed that agricultural land has expanded intensively at the expense of dense forest and woodland cover decline.

The increase in shrub bush land was maximum, 16.1% (70.36 km^2), from 2008 to 2018. From 1988 to 2018, the shrub bush land cover increased by 132.27 km^2 (35.28%) at a rate of 4.41 km^2 (1.17%) per year. The highest expansion of grassland in the study area was 18.88% (79.82 km^2) between 1998 and 2008. However, the increment was very small during 2008 and 2018, accounting for 7.25% (35.99 km^2). During the 1988–2018 period, grassland (grazing land) expansion was 43.47% (161.31 km^2) at an annual rate of 5.38 km^2 (1.45%) per year. Agricultural land (irrigated and rain fed crops) clearly showed a high expansion compared to the other land cover classes. Crop cultivation inside the park was absent in 1988; however, it started after 1993 and continued in 1998, 2008, and 2018, with extents of approximately 3%, 4.43%, and 5.48%, respectively. The highest expansion of cultivation was observed between 1993 and 1998, by 64.8 km^2, followed by 47.5% (30.78 km^2) from 1998 to 2008. However, the expansion was relatively small, 23.8% (22.78 km^2), between 2008 and 2018. From 1993 to 2018, cultivation increased by 118.36 km^2 at an annual rate of 3.94 km^2 per year (Tables 9 and 10). Water bodies: In three decades (1988–2018), water negatively changed by 13.29 km^2 (27.51%) at an annual rate of 0.44 km^2 (0.92%) per year. Bare land's highest expansion of change rate was 11.8% (3.78 km^2) during 1998 and 2008, followed by 10.08% (2.94 km^2) and 3.61% (1.3 km^2) from 1988 to 1998 and 2008 to 2018, respectively. In the whole study period, bare land expansion was 27.52% (8.02 km^2), with an annual rate of increase of 0.27 km^2 (0.92%) per year between 1988 and 2018 (Tables 9 and 10). However, based on the seasonal comparison of March 2018 and October 2018, bare land cover tremendously expanded from wet months to drier months (Figure 6). Consistent studies in Ethiopia quantified that bare land increased by 49.1%, whereas natural forest decreased by 35.76% from 1984 to 2015 (Gebrie et al., 2021). Likewise, in Malawi, bare land areas increased extremely as the expense of forest declined (Munthali et al., 2019). The conversion of woody vegetation to cultivation has been broadly reported in different areas of Ethiopia (Ewunetu et al., 2021; Takala et al., 2020; Anteneh et al., 2016) and Kenya (Erdogan et al., 2011; Maeda et al., 2010). Moreover, a study in semiarid Karamoja of Uganda and the MPA of South Africa showed expansion of crop cultivation and heightened encroachment of shrub bush land as the cost of woodland declined (Bailey et al., 2016; Egeru et al., 2014). From 1979 to 2017, Quirimbas National Park lost 41.67% of forest and changed to other human-made LULC (Mucova et al., 2018). In central Kenya, farmland and bare land increased by 160.45% and 73.2%, respectively, as a cost of forest decline (Maina et al., 2020). From 1957 to 2014, the forest area decreased by 83.8% (0.87 km^2 $year^{-1}$), while shrub, farmland and bare land expanded by 18.6% (0.23 km^2 $year^{-1}$), 57.7% (0.92 km^2 $year^{-1}$), and 0.114 km^2 $year^{-1,}$ respectively (Esa and Assen, 2017). Between 1986 and 2009, shrub land increased by 23.5% and agricultural land by 0.16 km^2 $year^{-1}$ (24.1%), while forestland decreased by 33.5% (Dinka and Chaka, 2019). In contrast to the present study, grassland and bare land declined while agricultural land increased (Andarge et al., 2020).

From 1988 to 2018, major LULC class transformation from and to highlighted grassland gained a large area from woodland (353.7 km^2) and subsequent shrub bush land (71.2 km^2). However, grassland gained negligible area from the rest of the land use/land cover classes. Similarly, agricultural land gained significant area from woodland (71.8 km^2), grassland (12.6 km^2), riparian vegetation (11.9 km^2), and shrub bush land (20.8 km^2). The highest loss was computed from woodland and shrub bush land class types during the studied period (Table 11).

Table 11. Major land cover classes of transformation (conversion) from and to KSNP (1988–2018).

Conversion (transition) class types		Area coverage	
Change from class 1988	Change to class 2018	km^2	%
Woodland	Shrub-bushland	174.3	15.0
Woodland	Grass land	353.7	30.5
Woodland	Agricultural land	71.8	6.2
Shrub-bushland	Grass land	71.2	18.0
Shrub-bushland	Woodland	134.8	30.3
Shrub-bushland	Agricultural land	20.5	9.7
Riparian forest	Shrub-bushland	11.5	12.9
Riparian forest	Woodland	40.1	45.0
Riparian forest	Agricultural land	11.9	6.9
Grass land	Agricultural land	12.6	2.8

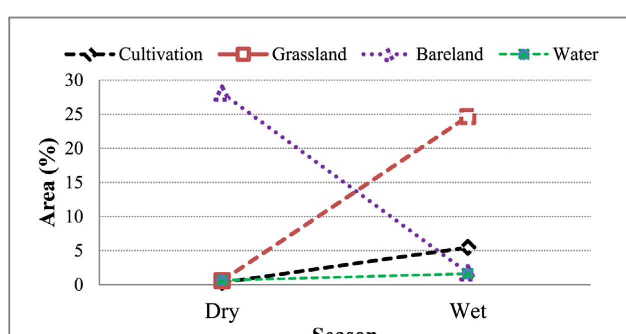

Figure 6. Seasonal land use/land cover class (bare land, cultivation, grassland, and water) cover change in Kafta Sheraro National Park (KSNP) in March and October 2018.

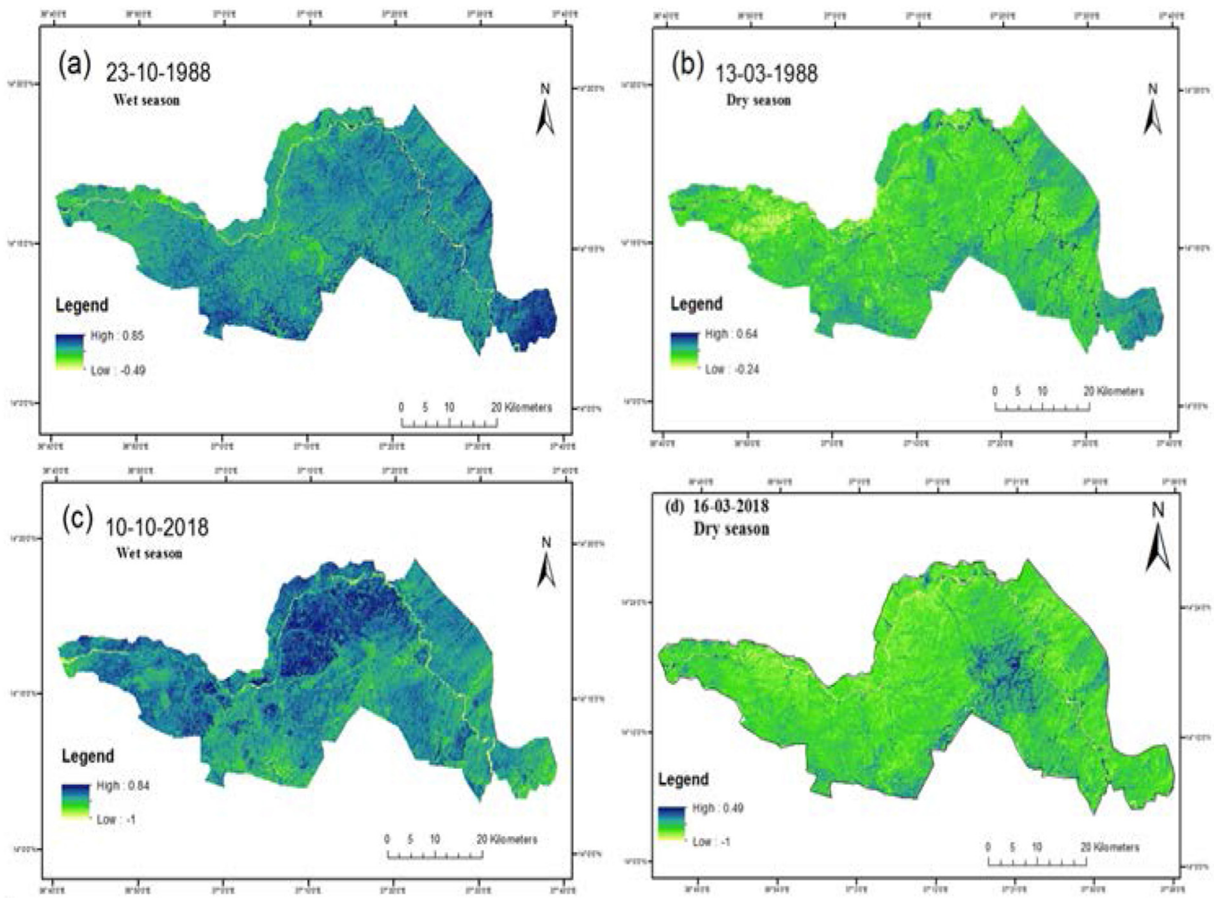

Figure 7. Seasonal variability in NDVI (greeness status) in Kafta-Sheraro National Park (KSNP) for the wet season (a and c) and dry season (b and d) during the 1988 and 2018 satellite images.

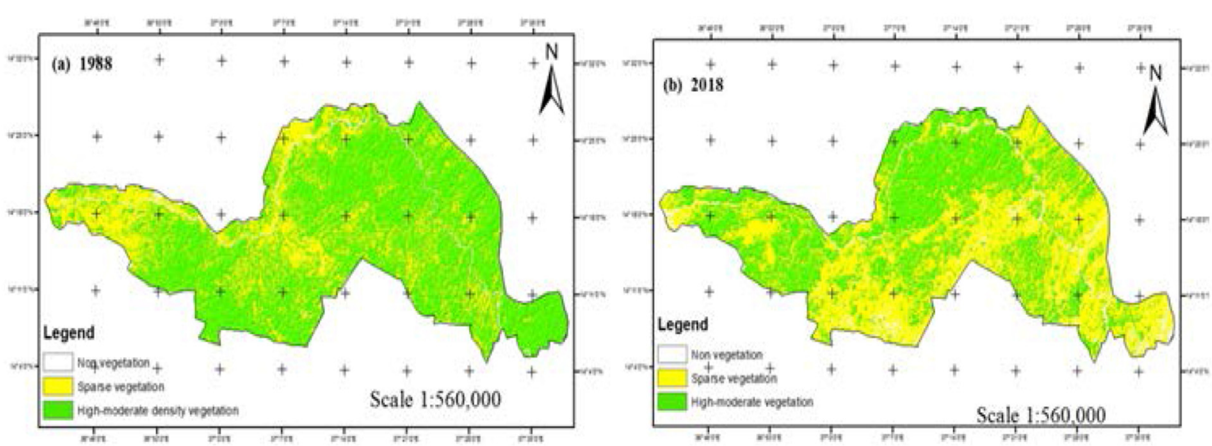

Figure 8. Vegetation cover change distribution of Kafta-Sheraro National Park in 1988 (a) and 2018 (b).

3.2.1. Seasonal LULC change

In addition to temporal variation in LULC change, some classes varied their proportion and rate of change seasonally (i.e., dry and wet seasons). Thus, the comparison between the wet season (October 2018) and dry season (March 2018) satellite images of LULC change classification of KSNP was computed (Figures 4 and 5). The results indicated that the land cover class of bare land increased by 26.3% (568.46 km^2) from the wet season toward the drier season because the total rain fed crop field and grazing areas were changed into bare ground during long dry months. In contrast, cultivation (rain-fed crops), grazing land, and water decreased by 5.15% (111.26 km^2), 24.06% (519.5 km^2), and 0.97% (21 km^2), respectively, from wet months to drier months. Bareland was very small in the wet season but increased toward drier months, whereas grassland and agriculture were relatively small in the dry season but increased in the wet season (Figure 6). The pronounced change in bare land occurred due to the harvesting of rainfed crops and dried and removed pasture during the prolonged dry months. According to (Msigwa et al., 2019), LULC change variation occurred between dry season irrigated crops and wet season rain fed crops. They suggested that during the dry season, bare land is increasing, while in the wet season, bare land is very small.

Table 12. Normalized difference vegetation index (NDVI) of land cover change (area in km^2 and %) in Kafta Sheraro National Park between 1988 and 2018.

Land cover class	1988		2018		2018–1988
	km^2	%	km^2	%	Change (km^2)
High-moderate density vegetation	1439.4	66.67	974.8	45.2	−464.6
Sparse vegetation	643.5	29.8	1071.6	49.6	+428.1
Nonvegetation (water &riverside sand)	76.115	3.5	112.6	5.2	+36.5
Total	2,159	100	2,159	100	....

3.3. Temporal and seasonal changes in NDVI

The seasonal variation in the average NDVI between wet and dry seasons was observed and reported in several semiarid areas (Amri et al., 2011; Ferreira et al., 2003). Illegal fire, extensive agriculture, charcoal production, and other related human-induced drivers of LULC change negatively affected the vegetation resources of the park. To detect vegetation cover changes over a thirty-year period, normalized difference vegetation index (NDVI) analyses of the 1988 and 2018 wet and dry season satellite sensors were utilized. Figure 7 indicates the NDVI threshold-based difference between the dry (mid-March) and wet (mid-October) months of 1988 and 2018. The pixel count of the wet season showed a higher NDVI value of 0.85 in 1988 and 0.84 in 2018 from June to mid-October; the park areas are dominated by vegetated woodland, shrubland, and riparian (Riversides) vegetation. During the dry season, from the end of December to the end of March, the maximum NDVI value was 0.64 in 1988 and 0.49 in 2018. During the dry season, dominant vegetated areas were concentrated on the sides of water points (hereafter Tekeze River sides and its tributary rivers) and the eastern riversides irrigated fruit plantations of the park. Our result concurred with a study in semiarid areas of Uganda, which indicated that the mean NDVI of the wet season was higher than that of the dry season (Egeru et al., 2014).

The present reclassification analysis of NDVI also showed a significant change in areas of vegetation cover (Figure 8 and Table 12). The high-moderate density vegetation cover in 1988 was approximately 66.67%. However, the magnitude of its cover in 2018 declined to 45.2%. In the entire period of 1988–2018, high- to moderate-density vegetation was reduced by 464.6 km^2. The sparse vegetation covered 29.8% of the total area of the park in 1988 but expanded to 49.6% in 2018. Sparse vegetation coverage increased by 428.1 km^2 from the total area of the park between 1988 and 2018. Moreover, the coverage of nonvegetation increased from 3.5% in 1988 to 5.2% in 2018. Nonvegetation showed an expansion of 36.5 km^2 from 1988 to 2018 (Table 12). The NDVI results also indicated a significant change in vegetation cover; the amount of high- to moderate-density vegetation cover declined by 21.47%, while sparse vegetation cover increased by 19.8% from the total area of KSNP. On the other hand, nonvegetation cover increased by 36.5 km^2 between 1988 and 2018. In agreement with the present study, the dense vegetation cover declined by 26.1%, whereas nonvegetation increased by 14.3 km^2 between 2000 and 2018 (Abera et al., 2020). In the Kafta humera district (surrounding the park), woodland vegetation converted by cropland leads to expanding bare ground during the dry season (Zewdie and Csaplovics, 2016).

3.4. Seasonal NDVI-precipitation/temperature relationship

According to the wet and dry season Landsat data, the interannual variation in NDVI during the 10-year period (2007–2016) was computed. The dry season mean NDVI indicated a significant decreasing trend ($p < 0.05$), while the wet season variation was nonsignificant over time. The dry season maximum mean NDVI value occurred in 2007 and 2008, while the minimum value occurred in 2016. In the wet season, the minimum and maximum mean NDVI values were 0.21 in 2012 and 0.33 in 2007, respectively (Figure 9a and b). In contrast, the rainfall did not show significant ($p > 0.05$) variation in the specified period (Figure 9c and d). The relationship between NDVI and climate variables (rainfall

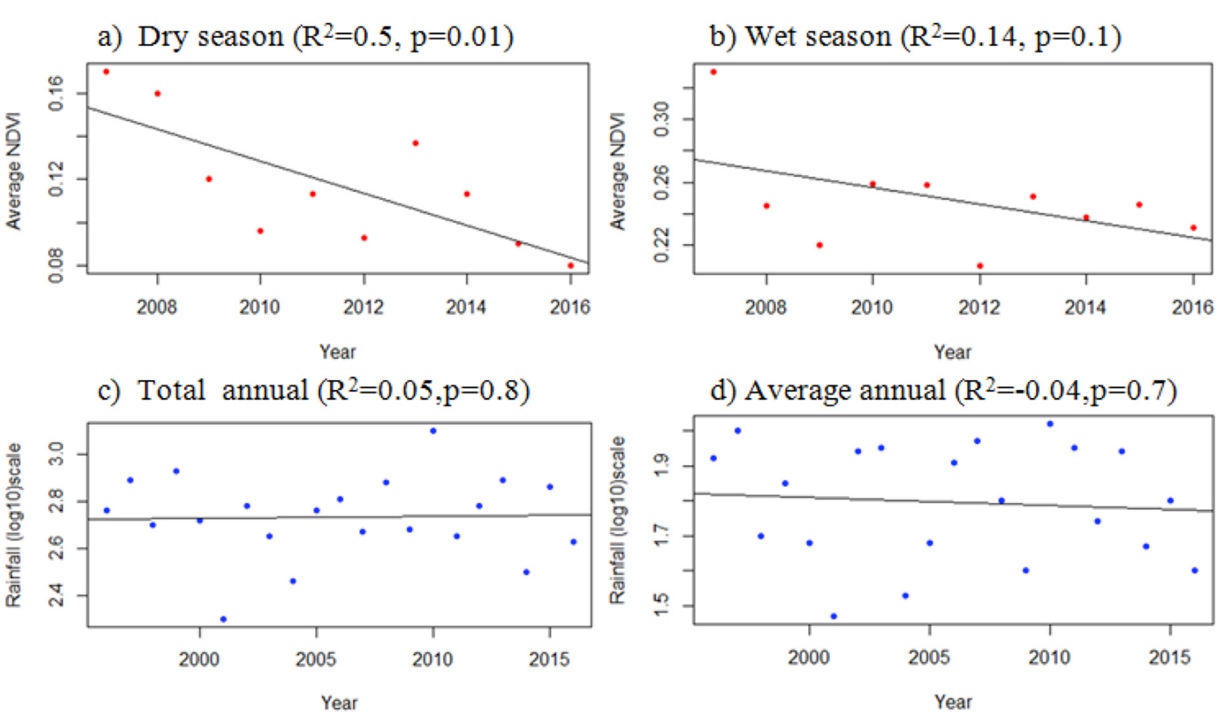

Figure 9. The interannual variation in the seasonal mean NDVI between 2007 and 2016 showed significant variation in the dry and wet seasons (a and b) (Source: Present study). However, the pattern of total annual rainfall (c) and average annual rainfall (d) between 1996 and 2016 did not significantly change over time for Kafta Sheraro National Park (ENMA, 2018).

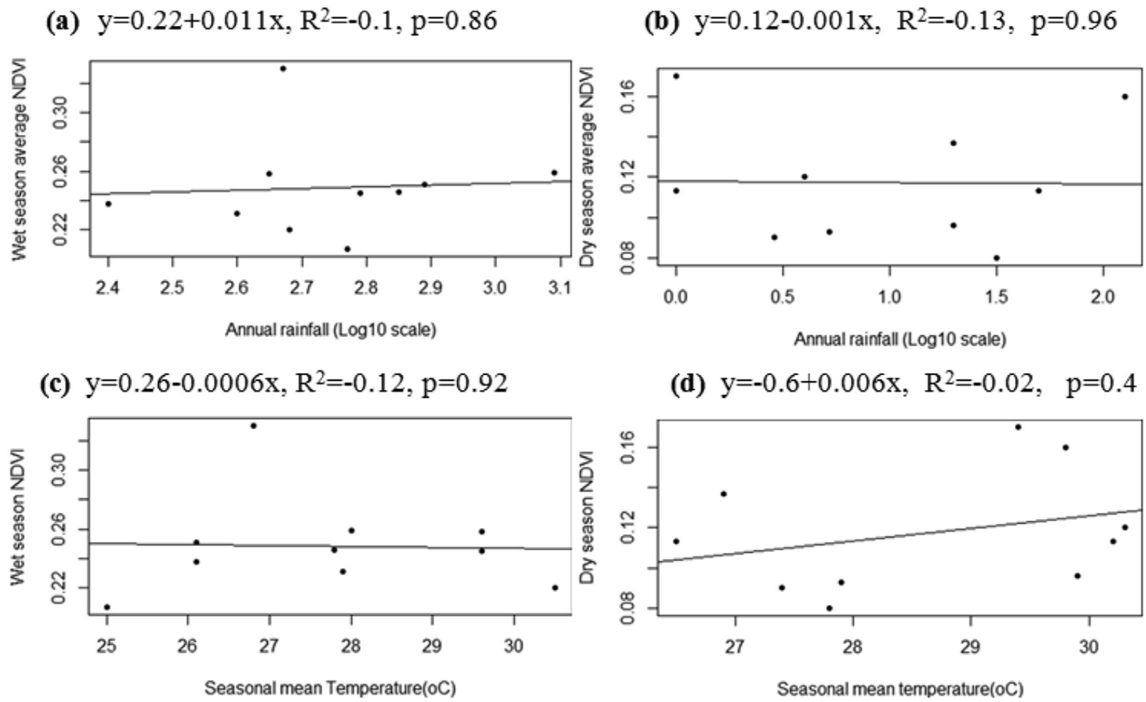

Figure 10. Regression analysis of the seasonal mean NDVI trend and relationship with (a and b) wet and dry season rainfall (mm) and temperature (°C) (c and d) between 2007 and 2016.

and temperature) was analyzed for a ten-year period (2007–2016) because satellite image data were absent before 2007 and some values of daily rainfall and temperature were missing. Figure 10a–d summarizes the statistical analysis between the seasonal mean NDVI, mean annual rainfall (value scale in log10 to fit NDVI values), and mean temperature between 2007 and 2016. Even if there was a change in seasonal rainfall and temperature, the correlation relationship of wet and dry season NDVI with these two climate variables was not statistically significant ($p > 0.05$). The variation and slight decreasing trends in NDVI might occur due to the dominant nature of the scattered woodland vegetation composition of the park and several activities of the local communities, such as extensive woodland conversion to cultivation and extinguishing of illegal fire and fuel wood collection. In line with our findings, vegetation cover change in Nechsar National Park was due to human-driven deforestation (Fetene et al., 2015). Similarly, temporal reduction of NDVI in dry land Ethiopia changed the woodland cover due to the expansion of cropland, settlements, and fuel wood harvesting (Zewdie and Csaplovics, 2016).

The variation in seasonal rainfall and temperature trends in the study period was not consistent with the mean NDVI trends in the wet and dry seasons. This directly reflects the influence of rainfall and temperature, which were not considered the main drivers of vegetation cover change in the KSNP. Due to limited local meteorological stations, a lack of advanced recording instruments and skilled manpower leads to low accuracy of climate variable data. Therefore, the statistical analysis revealed that precipitation and temperature were not considered the main drivers of vegetation dynamics; rather, human-induced factors were the major actors in the vegetation cover decline of the park. Moreover, dry season vegetation areas along the Tekeze Riversides are independent of annual rainfall, as they directly access water from the bank of the river. However, the seasonal decreasing trends of NDVI are more interlinked with increasing human driving activities, such as the conversion of woody vegetation to seasonal cultivation and bare land, loss of vegetation by fire, firewood collection, and charcoal production. Consistent with our study results in Africa, the Sahel also showed that human-induced activities increase vegetation degradation (Evans and Geerken, 2004). Moreover, however, Ethiopian dry land vegetation productivity is dominantly controlled by the availability of moisture (Hailu et al., 2015); the low correlation between precipitation and NDVI is due to the decline in vegetation cover (Li et al., 2004). This is an indication of a slight response of degraded woodland area to precipitation (Zewdie and Csaplovics, 2016).

In contrast to the present study, reports have shown that NDVI change (either increasing or decreasing) is driven by precipitation/temperature in arid and semiarid areas of Africa (Ghebrezgabher et al., 2020; Martiny et al., 2006) and in other countries, such as Spain, Iraq, and China (Naif et al., 2020; Chu et al., 2007; Fensholt et al., 2012; Pei et al., 2019; Sanz

Table 13. Socioeconomic general characteristics of the sampled households (N = 395).

Household characterstics	Categories	Calculated values
Gender	Male	74.0%
Age	–	Min: 22; mean: 44.7; max: 75 years
Ethnic category	Tigraway	86.0%
	Kunama	14.0%
Family size	2–5; 6–8	Min: 2; mean: 5; max: 8
Education status	Formal (1–12th grade)	74.2%
Resettlement status (1991–2002)	–	71.7%
Distance from settlement to park	5–10 km; 11–15 km; >15 km	Min: 6. 5; mean: 12.6; max: 21 km
Respondents alternative income		12.9%
Energy for cooking	Fuelwood	94.7%
Farmland holding size	1–3 ha; 4–7 ha; >7 ha	Min: 1; mean: 4.2; max: 10 ha
Crop use (home consumption and sale)	–	72.4%
Source of livelihood & income	Crop production	1 (rank)
Land tenure (land use permits)	Legal	86.0%

N = total number of the sampled households interviewed for this study; min = minimum; max = maximum.

Table 14. The main livelihood and economic activities ranked by respondents (N = 395[$]).

Activities	Number of respondents (n)	%
Crop production (rainfed and irrigated)	197	50.0
Livestock rearing	25	6.3
Mixed crop and livestock	173	43.7
Private and government employee	22	5.5
Self business	17	4.3
Fuelwood (charcoal and firewood collection)	5	1.3
Gold mining and aromatic resin collection	7	1.8

[$] The total number of respondents was 395; however, overcounts are predictable due to multiple responses of households to questions.

et al., 2021). NDVI controls the growth of vegetation conditions, temporal biomass accumulation, and changes (Zhao et al., 2014). The spatiotemporal variation in NDVI was determined by the variation in the temporal distribution of precipitation (Xia et al., 2014). On the other hand, the huge differences in the vegetation cover between the dry and wet seasons were due to climatological and anthropogenic effects (Al-Saady et al., 2015). Similarly, in the Gojeb district, Ethiopia, and the Three-North Shelter Forest of China, vegetation degradation is mainly influenced by both human-induced factors and rainfall variability (Huang and Kong, 2016; Dagnachew et al., 2020).

3.5. Local community perception of the drivers of LULC change

3.5.1. Demographic and socioeconomic information of the sampled households

The age of the sampled household heads (N = 395) ranged from 22 to 75 years old, with an average of 44.7 ± 13.7 (SD) years, and more than fifty percent of respondents' age category (22–41 years) was in the productive region. Approximately 74% of the sampled households were male. The household size ranged from two persons to 8 persons, with an average of ~5 persons. The farm size of the respondents varied from 1 to 10 hectares, with an average of 3.9 hectares. With respect to their education status, 74.2% of the respondents attended formal education, and 25.8% attended informal education (Table 13). Approximately three-fourths of the sampled households were engaged in crop production and mixed crops and livestock. However, a small portion of the respondents were involved only in livestock rearing and other additional activities coupled with farming. Crop production was ranked as the topmost important source of livelihood/income, followed by mixed crop and livestock farming in the districts (Table 14). The most important types of crops produced in the study area were rainfed: *Sesamum indicum*, *Sorghum bicolor*, *Eleusine coracana*, *Eragrostis tef*, and *Zea mays* L., whereas irrigated crops included *Muza species*, *Mangifera indica*, *Carica papaya*, *Allium cepa*, *Allium sativum*, *Solanum tuberosum*, and *Capsicum annuum*.

3.5.2. Local community response to trends of LULC variables

Local community perception of major LULC change types and other associated variables of change showed statistical significance ($p < 0.001$). The participants were well aware that woodland and riparian forest (Tekeze River side vegetation of the park) significantly declined in the whole study period ($p < 0.001$). The local communities provided confidential evidence for the decline of approximately 90.3% woodland and 88.7% riparian vegetation of KSNP and its surroundings. In contrast, approximately 57.3% of the respondents recognized that the distance from the water source to the settlement showed constant trends. However, agricultural land, grazing area (grassland), bare land, resettlement, and road access to the park significantly increased throughout the studied periods ($p < 0.001$) (Figure 11).

3.5.3. Main (immediate) drivers of LULC changes in KSNP

The drivers of LULC change were both proximate and underlying (Munthali et al., 2019; Bewket and Abebe, 2013). For this discussion, more emphasis is given to the proximate drivers of LULC change. During the surveyed period, the participants identified 13 pronounced factors as key drivers of the observed LULC change in KSNP. The expansion of legal and illegal settlements, cultivated land, illegal fire following encroachment by cultivation, seasonal grazing, firewood collection, and traditional gold mining were prioritized as the top significantly ($p < 0.001$) ranked drivers (Table 15). Likewise, from key informant interviews and focus group discussions (FGDs), similar feedbacks were also recorded, and they were strengthened; expansion of settlements and agriculture, firewood collection, charcoal production, and land tenure (administration) problems were identified as the main causes of LULC change in the study area.

These main drivers were generated by a scarcity of resources in the moderate- and high-altitude areas of the region following resettlement from dense to less populated areas, low awareness regarding the

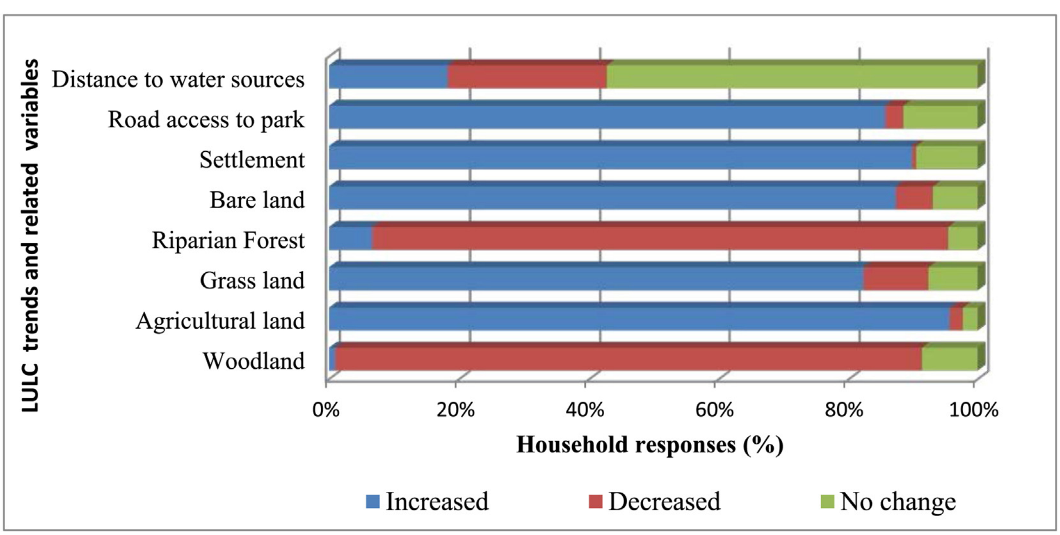

Figure 11. Respondents' awareness of the trend of LULC and related variables (N = 395).

Table 15. Main drivers of LULC change recognized by local communities' perceptions in Kafta Sheraro National Park (N = 395[1, 2, * and $]).

Recognized land use land cover change drivers	Number of households choosen the drivers*				Total [1] score	Ranking[2] ratio
	Rank (1)	Rank (2)	Rank (3)	Rank (4)		
Legal and illegal resettlement	156	94	45	15	1011	0.18
Expansion of cultivated land	104	84	61	16	806	0.14
Illegal fire	83	74	50	19	673	0.12
Expansion of grazing land	74	65	61	39	652	0.11
Firewood collection	59	46	63	46	546	0.09
Traditional gold mining	37	47	58	39	444	0.08
Charcoal production	35	56	43	41	435	0.07
Land administration problem	29	51	37	25	368	0.06
Natural resin collection	20	35	28	27	268	0.047
Ethio-Eritrean war (civil war)	14	19	18	16	165	0.030
Drought	11	21	11	16	145	0.025
Eritrean community intervention	7	22	9	13	125	0.022
Permanent and seasonal road	0	6	11	13	53	0.009
Σ weight total - - - -					**5691**	–

[1] Weight = $R_4C_1 + R_3C_2 + R_2C_3 + R_1C_4$.
[2] Index = $R_4C_1 + R_3C_2 + R_2C_3 + R_1C_4/\Sigma\, R_4C_1 + R_3C_2 + R_2C_3 + R_1C_4$ (5691).
[*] The negative importance of drivers decreases from Rank (1) to Rank (4).
[$] The total number of respondents was 395; however, overcounts are predictable due to multiple responses of households to questions.

environmental benefits of natural resources, lack of access to renewable energy sources (i.e., solar energy and electric cities) and high poverty. According to the household survey, focus group discussion and key informant interviewers' resettlement schemes by the government and a few illegally were highly expanded in the study area between 1991 and 2003. From the household response, approximately 71.7% were resettlers (Table 13). Due to the program, new settlement communities, namely, Tekeze, Maytemen, Maykeyh, Fre-Selam, Wuhedet, and Mayweyni, were established near KSNP. Similar studies in Ethiopia showed that resettlement programs have brought significant LULC and massive clearance of forests and depletion of much natural vegetation cover in Hawa Galan and Chewaka districts, Oromia (Yadeta et al., 2022; Abera et al., 2020), Gelda district, Amhara (Esa and Assen, 2017), and Esira district of the South region (Mamude et al., 2021).

The majority of the sampled households (~94.7%) utilized wood and wood products for cooking (Table 13). These activities led to the destruction of dominant woodland outside and inside the KSNP. As stated by the focus group discussion and key informant interviews, the woodland of the park is not only used as source energy but also used as a source of alternative income by the local communities. This result is in line with Central Rift Valley, Ethiopia (Bekele et al., 2019), Gelana, Ethiopia (Asmame and Abegaz, 2017), Dedza, Malawi (Munthali et al., 2019), and Quirimbas National Park, Mozambique (Mucova et al., 2018), which revealed that fire wood collection and charcoal making were the main drivers of LULC change.

The area has great potential for nonrenewable natural resources, and traditional gold mining is a common activity that negatively changes the land cover of the study site (Figure 12a). The activity of gold mining also leads to a drift population from other areas toward the mine sites and increased settlements in the whole surrounding area of KSNP, and they even constructed temporary structures as a place of residence inside the park. According to vegetation surveyed by KSNP, the above listed activities destroy the natural vegetation by uprooting the plants' root profile and are an approximate cause for extinguishing illegal fire

Figure 12. Traditional gold mining activities (a) preparing land for irrigated planting (b) and cultivations of banana (c) and cereal crops (d) along the Tekeze riversides of Kafta-Sheraro National Park (Photo by Fitsum Temesgen, 2018–2019): Remark: The photo (Figure 12c) refers to the corresponding author while conducting field work (identifying land/use cover classes of rainfed crops & ground truth recording).

(Temesgen and Warkineh, 2020). Gold mining coupled with an expansion of settlement in East Cameron had a negative impact on natural vegetation (Kamga et al., 2020). Furthermore, mining activities in Ghana had a pronounced impact on the loss of vegetation (Garai and Narayana, 2018; Prosper et al., 2015).

Based on socioeconomic and field observation data, illegal fire is another proximate significant driver of LULC change in the KSNP. The dry season fire was extinguished for a different purpose by three agents: (1) farmers, (2) *Boswellia papyrifera* resin collectors and (3) traditional gold miners. The local community farmers prepared the land for cultivation through the destruction of woodlands by burning, while resin collectors and traditional gold miners used fire for daily food preparation. All the agents destroyed the valuable natural resources of the park, which led to wildlife migration outside the park. Detailed human-induced fire hazards related to LULC change reports are limited in Ethiopia; however, a consistent study in hot spot tropical countries of Brazil, the Serengeti ecological unit, and Cameroon for an 18-month period daily fire observation record indicated a direct relationship between the occurrence of fire and LULC change (Eva and Lambin, 2000). On the other hand, a study in central Spain of frequently burned areas showed that pine woodland coverage decreased while shrubland encroachment increased (Viedma et al., 2006). Similar reports also indicated that human-induced fire made a great contribution to increasing the destruction or loss of vegetation, which is a direct expansion of bare land areas (Prosper et al., 2015).

In addition to the local community pressure on natural resources, civil war and border conflicts are additional factors in Ethiopia. According to the household, focus group discussion, and key informant interviews, the Ethio-Eritrea war of 1998/99 dominantly destroyed the socioeconomic features of the Tigray region, including the uncounted vegetation and wildlife resources in and around KSNP. During the war period, the military mechanization of the Eritrean troop crossed the park area and destroyed the natural resources. Our result was consistent with the Syrian conflict (2011–2018), which significantly and negatively influenced environmental resources (Mohamed et al., 2020). Similarly, the civil war of Sri Lanka (1983–2009) affected forest reserves and protected areas of the country (Rathnayake et al., 2020). The Civil War of Sierra Leones (1991–2002) also caused the contraction of the Kono district forest cover structure and its spatial extent (Wilson and Wilson, 2012).

3.5.4. Socioeconomic characteristics vs respondents' awareness of drivers

Logistic regression was applied to analyze ($p < 0.05$) the top four recognized drivers, namely, resettlement, expansion of agriculture, fire, and expansion of grazing land at the household level (Table 16). Seven demographic and socioeconomic explanatory (independent) variables were utilized for the whole analysis. The results of the analysis indicated that settlement duration ($p = 0.01$) and the distance from the settlement area to KSNP ($p = 0.04$) significantly and negatively influenced the sampled households' degree of awareness of the expansion of agriculture and grazing land. Additionally, respondents' high awareness of the expansion of cultivated land, settlement, illegal fire, and expansion of grazing was influenced significantly ($p = 0.001$) and negatively by the education level of the interviewees. The perception of respondents of the expansion of grazing land and expansion of settlement (resettlement) was also negatively influenced by individual household size and agricultural land size occupied ($p = 0.045$). The remaining explanatory variables, such as age category, gender, number of families, and the landholding size of respondents, did not significantly influence the perception of respondents of the four drivers of LULC change listed below (Table 16).

3.5.5. LULC change impact implication on KSNP sustainability

Understanding and evaluating the spatial and temporal LULC changes in natural vegetation inside and outside the KSNP and the negative contribution of the local community to these changes are significant. According to the classified image, changes were detected in different land cover classes between 1988 and 2018, which indicated that dominant woodland and riparian forest transformed into cultivation, grazing land, and bare land. As a consequence, the land surface was left with scattered vegetation and bare ground, which immediately showed how the natural vegetation (plant biodiversity) was lost over time and limited the habitat range of the wildlife. Moreover, the change in woodland was expanding into farmland, leading to encroachment of the African elephant habitat and creating a major challenge for their free movement.

Similarly, our questionnaire assessment also confirmed that the range of wildlife before 30 years was anywhere in the park area. Recently, the suitable habitats for wildlife have shrunk and collapsed in specific areas in the park because agricultural expansion coupled with the extinguishing of illegal fire has progressively increased. Second, the encroachment of livestock, firewood and charcoal collectors and traditional gold miners

Table 16. The impacts of household demographic and socioeconomic status on attitudes toward the top four recognized drivers of LULC change in Kafta Sheraro National Park.

Independent variables	*B*	*S.E*	*Wald*	*p value*
1. Expansion of cultivated land (driver-dependent variable)				
Age	0.62	0.45	1.87	0.17
Gender (1 = male)[a]	0.20	0.31	0.42	0.52
Education level (0 = Informal)[a]	–	–	–	–
Education level (1 = 1–8 grade)*	−4.78	1.08	19.43	0.00
Education level (2 = 9–12 grade)	0.05	0.41	0.02	0.89
Household size	−0.73	0.41	3.08	0.08
Settlement duration*	−0.79	0.31	6.60	0.01
Agricultural land size	−0.41	0.56	0.54	0.46
Distance from settlement to park	−0.22	0.29	0.58	0.44
2. Resettlement (driver-dependent variable))				
Age	−0.44	0.42	1.10	0.29
Gender (1 = male)[a]	−0.47	0.29	2.70	0.10
Education level (0 = Informal)[a]	–	–	–	–
Education level (1 = 1–8 grade)*	−2.10	0.54	15.21	0.00
Education level (2 = 9–12 grade)	−0.09	0.41	0.05	0.82
House hold size	0.55	0.38	2.12	0.14
Settlement duration	0.22	0.29	0.60	0.44
Agricultural land size*	−1.23	0.66	3.46	0.045
Distance from settlement to park	0.18	0.27	0.43	0.51
3. Human induced fire (driver-dependent variable)				
Age	0.25	0.44	0.34	0.56
Gender (1 = male)[a]	0.24	0.30	0.64	0.42
Education level (0 = Informal)[a]	–	–	–	–
Education level (1 = 1–8 grade)*	−3.31	0.64	26.74	0.00
Education level (2 = 9–12 grade)	0.16	0.41	0.15	0.70
House hold size	−0.05	0.39	0.02	0.89
Settlement duration	0.17	0.30	0.33	0.56
Agricultural land size	−0.29	0.54	0.28	0.59
Distance from settlement to park	−0.22	0.25	0.61	0.43
4. Expansion of grazing (driver-dependent variable))				
Age	0.57	0.45	1.61	0.20
Gender (1 = male)[a]	0.03	0.30	0.01	0.93
Education level (0 = Informal)[a]	–	–	–	–
Education level (1 = 1–8 grade)*	−3.83	0.82	21.97	0.00
Education level (2 = 9–12 grade)	0.31	0.41	0.59	0.44
House hold size*	−0.77	0.42	3.45	0.045
Settlement duration	−0.02	0.31	0.01	0.93
Agricultural land size	0.23	0.58	0.16	0.69
Distance from settlement to park*	−0.56	0.29	3.78	0.04

* = significant at 5% (0.05), S. E = standard error; B = coefficient of explanatory variable.

[a] Female and informal education set as zero (i.e., References variables).

led to disturbance and displaced wildlife from the long existing habitat and shifted to new habitat patches. The increasing demand of the local communities for irrigated crop cultivation, livestock grazing, water for home and livestock consumption, and other resource utilization were obstacles to wildlife movement and access to water, especially during the dry season. Such activities increased the conflict between elephants and humans. Moreover, the shift of the riparian forest LULC class into farmland (irrigated area) around water points is the immediate cause for wildlife free movement and blocks water access. Most likely, wildlife is forced to migrate outside the park boundary even far from neighboring countries. This report concurs with Ellis' (2006) study that LULC change dramatically reduced biodiversity. Similarly, in the northern highlands of Ethiopia, LULC change was reported as an indication of plant and wildlife species loss (Asmame and Abegaz, 2017). A study in PAs of Mexico also indicated a reduction in temperate and tropical vegetation cover threatened to the whole biodiversity of the site (Sancheza Reyes et al., 2017). A recent study in Bale Mountain National Park revealed that the decreasing trends of grassland and forestland while increasing farmland LULC led to increased habitat fragmentation and reduced the size and loss of available core area for the existing core-dependent endemic wildlife species (Muhammed and Elias, 2021). Furthermore, the expansion of agriculture threatens elephant habitats and increases competition for resources between humans and elephants (Sintayehu and Kassaw, 2019). The decline in woody savanna in Tarangire National Park was also an indication of a threat to wildlife conservation (Mtui et al., 2017).

4. Conclusion and recommendation

The results of a three-decade (1988–2018) study indicated that intensive and extensive LULC changes were observed in Kafta Sheraro National Park (KSNP). The proportional change in the park was used to determine the total LULC types in three different periods. Thus, recognizing and mapping LULC is important in planning continuous studies on natural resource management. The most important change was observed in the decline of woodland and riparian forest from 1,251.9 km^2 and 83.77 km^2 in 1988 to 884 km^2 and 44.31 in 2018, respectively. In contrast, agricultural land expanded from 64.79 km^2 in 1998 to 118.35 km^2 in 2018 from the total park area. LULC classes of shrub bush land, grassland, water bodies, and bare land have shown relatively moderate changes. The serious degradation of woodland and riparian vegetation of the park resulted in the encroachment of shrub bush land and an increase in sparse vegetation cover ground (bare land), cultivated land, and grazing land. The major depletion trend was observed from woodland to rainfed crop cultivation and from riparian vegetation to irrigated land. In general, the period between 1998 and 2008 showed the highest change compared with the other two periods (i.e., 1988 to 1998 and 2008 to 2018). This large change was possible due to the high resettlement program around the PA in that period relative to the other periods. The seasonal change in grassland and cultivation enormously expanded from the drier season to the wet season, whereas bare land showed pronounced expansion from wet months to drier months (Figure 6). The results of the NDVI analysis indicated that the dense woodland and riverside vegetation decreased from 66.67% in 1988 to 45.2% in 2018, while nonvegetation increased from 3.5% in 1988 to 5.2% in 2018. Based on field observations and interviews with local people, the gradual change in the vegetation cover of the park was mainly driven by increasing human-induced pressure on the natural resources. However, our results indicated that rainfall and temperature were not considered the main drivers of the extensive change in vegetation cover in the KSNP. The major habitat change factors are expansion of settlement and riverside/rainfed cultivation, human-induced fire, grazing, firewood collection, traditional gold mining, charcoal production, land administration problems, and natural resin collection, which degrade the wildlife habitat and limit their movement routes. The increasing trend of LULC change directly and negatively influences wildlife habitats, as the area is known home to African elephants and other wild animals.

Therefore, it is paramount to detect LULC changes and current environmental features and consider these features for each land use class in terms of revealing the feasibility of the land use potential in the study districts. Understanding the past and present LULC change drivers that are interlinked with the livelihood of local communities is essential. Manage and exclude newly opened settlements in natural forest areas and consider water resources, agricultural areas, and settlement areas when planning sustainable natural resource management in the area. Attention should be given to the sustainable conservation of park biodiversity by encouraging community participation in conservation practices, preparing awareness creation programs, and controlling all illegal activities practiced in and around KSNP. Furthermore, this study provides baseline information for setting effective land use planning and advanced management options for park sustainability. Natural structural features of the district area map for each land use should be located by local administrators for future forest and wild animal management. Fourteen percent (Table 13) of the local residents had unclear land rights (i.e., no legal land permit) and misbalanced access to land, which causes uncontrolled expansion of agriculture unless uniformly secured land rights are recommended to all households to minimize illegal expansion of farming and related issues.

Declarations

Author contribution statement

Fitsum Temesgen Hailemariam, Msc; Bikila Warkineh Dullo, Assistance Prof; Alemayehu Hailemicael Mesgebo, Assistance Prof.: Conceived and designed the experiments; Performed the experiments; Analyzed and interpreted the data; Contributed reagents, materials, analysis tools or data; Wrote the paper.

Funding statement

This work was supported by the Ethiopian Wildlife Conservation Authority (Enhanced Management and Effectiveness of Ethiopia's Protected Area Estate Project. Project No: 00103276.

Data availability statement

Data included in article/supp. material/referenced in article.

Declaration of interest's statement

The authors declare no competing interests.

Additional information

No additional information is available for this paper.

Acknowledgements

We greatly thank the Ethiopian wildlife conservation authority for permitting this research. We would also like to thank the KSNP scouts and the local community of the districts for supporting the field study and responding to questions.

References

Abera, A., Yirgu, T., Uncha, A., 2020. Impact of resettlement scheme on vegetation cover and its implications on conservation in Chewaka district of Ethiopia. Environ. Syst. Resour. 9 (2), 17.

Abyot, Y., Berhanu, G., Solomon, A., Ferede, Z., 2014. Forest cover change detection using remote sensing and GIS in Banja district, Amhara region, Ethiopia. Int. J. Environ. Monit. Anal. 2, 354–360.

Agidew, A., Singh, K.N., 2017. The implications of land use and land cover changes for rural household food insecurity in the Northeastern highlands of Ethiopia: the case of the Teleyayen subwatershed. Agric. Food Secur. 6 (56), 1–14.

Alawamy, J.S.S.K., Balasundram, A., Hanif, H., Sung, C.T., 2020. Detecting and analyzing land use and land cover changes in the region of Al-jabal Al-Akhdar, Libya using time-series landsat data from 1985 to 2017. Sustainability 12 (4490), 24.
Alemu, B., Garedew, E., Eshetu, Z., Kassa, H., 2015. Land use and land cover changes and associated driving forces in north western Lowlands of Ethiopia. Int. Res. J. Agric. Sci. Soil Sci. 5 (1), 28–44.
Al-Saady, Y., Merkel, B., Al-Tawash, B., Al-Suhail, Q., 2015. Land use and land cover (LULC) mapping and change detection in the Little Zab river basin (LZRB), Kurdistan region, NE Iraq and NW Iran. Freiberg Online Geosci. 43, 32.
Amri, R., Zribi, M., Lili-Chabaane, Z., Duchemin, B., Gruhier, C., Chehbouni, A., 2011. Analysis of vegetation behavior in a North African semiarid region, using SPOT-vegetation NDVI data. Remote Sens. 3, 2568–2590.
Andarge, A., Atzberger, C., Bauer, T., Kassaw, S., Mansberger, R., 2020. Analysis of land cover change in Gozamin district, Ethiopia: from remote sensing and DPSIR Perspectives. Sustainability 12 (4534), 1–25.
Anteneh, M., Assen, M., Nicolau, M.D., 2016. Patterns, causes and consequences ofLULC dynamics in the Gumara watershed of Lake Tana basin, Northwestern Ethiopia. Environ. Syst. Res. 5 (8), 1–12.
Asmame, B., Abegaz, A., 2017. Land use/land cover changes and their environmental implications in the Gelana sub-watershed of Northern highlands of Ethiopia. Environ. Syst. Res. 6 (7), 12.
Bailey, K.M., McCleery, R.A., Binford, M.W., Christa, Z., 2016. Land-cover change within and around protected areas in a biodiversity hotspot. J. Land Use Sci. 11 (2), 154–176.
Bekele, A., Yalden, D.W., 2013. Mammals of Ethiopia and Eritrea. Addis Abeba University press. Ethiopia 365p.
Bekele, B., Wu, W., Yirsaw, E., 2019. Drivers of land use-land cover changes in the Central Rift Valley of Ethiopia. Sains Malays. 48 (7), 333–1345.
Beresford, A.E., Buchanan, G.M., Phalan, B., Eshiamwata, G.W., Balmford, A., et al., 2018. Correlation of long-term land-cover change and protected area performance at priority conservation sites in Africa. Environ. Conserv. 45 (1), 49–57.
Berihun, M.L., Tsunekawa, A., Haregeweyn, N., Meshesha, D.T., Adgo, E., et al., 2019. Exploring land use/land cover changes, drivers and their implications in contrasting agro-ecological environments of Ethiopia. Land Use Pol. 87, 104052.
Bewket, W., Abebe, S., 2013. Land-use and land-cover change and its environmental implications in a tropical highland watershed, Ethiopia. Int. J. Environ. Stud. 70 (1), 126–139.
Bilgili, B.C.O., Satir, V., Muftuoglu, M., Ozyavuz, A., 2014. Simplified method for the determination and monitoring of green areas in urban parks using multispectral vegetation indices. J. Environ. Prot. Ecol. 15 (3), 1059.
Birhane, E., Ashfare, H., Fenta, A.A., Hishe, H., Gebremedhin, M.A., Wahed, G.H., Solomon, N., 2018. Land use landcover changes along topographic gradients in Hugumburda national forest priority area, Northern Ethiopia. Remote Sens. Appl. Soc. Environ. 13, 61–68.
Burgi, M. Bieling, C. von, K. Hackwitz, et al., 2017. Processes and driving forces in changing cultural landscapes across Europe. Landsc. Ecol. 32 (11), 2097–2112.
Butchart, S.H.M., Walpole, M., Collen, B., Van Strien, A., Scharlemann, J.P.W., Almond, R.E.A., Watson, R., 2010. Global biodiversity: indicators of recent declines. Science 328 (5982), 1164–1168.
Butsic, V., Baumann, M., Shortland, A., Walker, S., Kuemmerle, T., 2015. Conservation and conflict in the Democratic Republic of Congo: the impacts of warfare, mining, and protected areas on deforestation. Biol. Conserv. 191, 266–273.
Chander, G., Markham, B.L., Helder, D.L., 2009. Summary of current radiometric calibration coefficients for Landsat MSS, TM, ETM^{+}, and EO-1 ALI sensors. Remote Sens. Environ. 113, 893–903.
Chavez, P.S., Berlin, G.L., Sowers, L.B., 1982. Statistical method for selecting Landsat MSS ratios. J. Appl. Photogr. Eng. 8 (1), 23–30.
Cheruto, M.C., Kauti, M.K., Kisangau, P.D., Kariuki, P., 2016. Assessment of land use and land cover change using GIS and remote sensing techniques: a case study of Makueni County, Kenya. J. Remote Sens. GIS 5, 175.
Chu, D., Lu, L., Zhang, T., 2007. Sensitivity of normalized difference vegetation index (NDVI) to seasonal and interannual climate conditions in the Lhasa area, Tibetan plateau, China. Arctic Antarct. Alpine Res. 39 (4), 635–641.
Cochran, W.G., 1977. Sampling Techniques, third ed. John Willey and Sons, New York, p. 428.
Coetzee, B.W.T., Gaston, K.J., Chown, S.L., 2014. Local scale comparisons of biodiversity as a test for global protected area ecological performance: a meta-analysis. PLoS One 9, e105824.
Congalton, R.G., Green, K., 2009. Assessing the Accuracy of Remotely Sensed Data: Principles and Practices, second ed. Lewis Publishers, Boca Raton.
Coppin, P., Jonckheere, I., Nackaerts, K., Muys, B., 2004. Digital change detection methods in ecosystem monitoring: a review. Int. J. Remote Sens. 25 (9), 1565–1596.
Dagnachew, M., Kebede, A., Moges, A., Abebe, A., 2020. Effects of climate variability on normalized difference vegetation index (NDVI) in the Gojeb river catchment, Ethiopia. Adv. Meteorol. 1–16. Article ID 8263246.
DeFries, R., Hansen, A., Newton, A.C., Hansen, M.C., 2005. Increasing isolation of protected areas in tropical forests over the past twenty years. Ecol. Appl. 15, 19–26.
Dejene, T., Lemenih, M., Bongers, F., 2013. Manage or convert boswellia woodlands? Can frankincense production pay off? J. Arid Environ. 89, 77–83.
Dinka, M.O., Chaka, D.D., 2019. Analysis of land use/land cover change in Adei watershed, Central Highlands of Ethiopia. J. Water Land Dev. 41 (4-6), 146–153.
Duraisamy, V., Bendapudi, R., Jadhav, A., 2018. Identifying hotspots in land use land cover change and the drivers in a semiarid region of India. Environ. Monit. Assess. 190 (535), 21p.
Dwivedi, R.S., Sreenivas, K., Ramana, K.V., 2005. Land-use/land-cover change analysis in part of Ethiopia using Landsat Thematic Mapper data. Int. J. Remote Sens. 26 (7), 1285–1287.
Egeru, A., Wasonga, O., Kyagulanyi, J., Majaliwa, G.J.M., MacOpiyo, L., Mburu, J., 2014. Spatiotemporal dynamics of forage and land cover changes in Karamoja subregion, Uganda. Pastoralism: Research, Policy, and Practice 4 (6), 1–21.
Ellis, E., 2006. Land use and land cover change. In: Cleveland, C.J. (Ed.), Encyclopedia of Earth. Environmental Information Coalition, National Council for Science and the Environment. http://www.eoearth.org/article/Land use & cover change.
Erdogan, H.E., Pellikka, P.K.E., Clark, B., 2011. Modeling the impact of land-cover change on potential soil loss in the Taita Hills, Kenya, between 1987 and 2003 using remote-sensing and geospatial data. Int. J. Remote Sens. 32, 5919–5945.
Esa, E., Assen, M., 2017. Land use/cover dynamics and its drivers in Gelda catchment, Lake Tana watershed, Ethiopia. Environ. Syst. Res. 6 (4), 1–13.
ENMA (Ethiopian National Meteorology Agency), 2018. Rainfall and Temperature Data (1996-2016), Addis Ababa, Ethiopia.
Eva, H., Lambin, E.F., 2000. Fires and land-cover change in the tropics: a remote sensing analysis at the landscape scale. J. Biogeogr. 27, 765–776.
Evans, J., Geerken, R., 2004. Discrimination between climate and human-induced dryland degradation. J. Arid Environ. 57, 535–554.
Ewunetu, A., Simane, B., Teferi, E., Zaitchik, B.F., 2021. Land cover change in the blue nile river headwaters: farmers' perceptions, pressures, and satellite-based mapping. Land 10 (68), 1–25.
Fan, F., Weng, Q., Wang, Y., 2007. Land use land cover change in Guangzhou, China, from 1998 to 2003, based on Landsat TM/ETM+ imagery. Sensors 7, 1323–1342.
FAO, 2011. The State of the World's Land and Water Resources for Food and Agriculture (SOLAW)-managing Systems at Risk. Earthscan, London. http://www.fao.org/docrep/03/i1688e/i1688e01. Accessed 10 May 2021.281p.
Fensholt, R., Langanke, T., Rasmussen, K., Reenberg, A., Prince, S.D., Tucker, C., et al., 2012. Greenness in semiarid areas across the globe 1981-2007-an Earth Observing Satellite based analysis of trends and drivers. Remote Sens. Environ. 121, 144–158.
Ferreira, L.G., Yoshioka, H., Huete, A., Sano, E.E., 2003. Seasonal landscape and spectral vegetation index dynamics in the Brazilian Cerrado: an analysis within the Large-Scale Biosphere-Atmosphere Experiment in Amazônia (LBA). Remote Sens. Environ. 87, 534–550.
Fetene, A., Hilker, T., Yeshitela, K., Prasse, R., Cohen, W., Yang, Z., 2015. Detecting trends in Landuse and landcover change of nech sar national park, Ethiopia. Environ. Manag. 11.
Garai, D., Narayana, A.C., 2018. Land use/land cover changes in the mining area of Godavari coal fields of Southern India. Egypt. J. Remote Sens. Space Sci. 21, 375–381.
Garedew, E., Sandewall, M., Soderberg, U., Campbell, B., 2009. Land-use and land-cover dynamics in the central rift valley of Ethiopia. Environ. Manag. 44 (4), 683–694.
Garrard, R., Kohler, T., Price, M.F., Byers, A.C., Sherpa, A.R., Maharjan, G.R., 2016. Land use and land cover change in Sagarmatha national park, a world heritage site in the himalayas of eastern Nepal. Mt. Res. Dev. 36 (3), 299–310.
Gebreslassie, H., 2014. Land use-land cover dynamics of huluka watershed, Central Rift valley, Ethiopia. Int. Soil Water Conserv. Res. 2, 25–33.
Gebrie, D., Satishkumar, B., Ayenew, T., 2021. Evaluation of the status of land use/land cover change using remote sensing and GIS in Jewha Watershed, North eastern Ethiopia. SN Appl. Sci. 3 (501), 1–10.
Geldmann, J., Barnes, M., Coad, L., Craigie, I.D., Hockings, M., Burgess, N.D., 2013. Effectiveness of terrestrial protected areas in reducing habitat loss and population declines. Biol. Conserv. 161, 230–238.
Ghebrezgabher, M.G., Yang, T., Yang, X., Sereke, T.E., 2020. Assessment of NDVI variations in responses to climate change in the Horn of Africa. Egypt. J. Remote Sens. Space Sci. 23, 249–261.
Grinblat, Y., Kidron, G.J., Karnieli, A., Benenson, I., 2015. Simulating land-use degradation in West Africa with the ALADYN model. J. Arid Environ. 112, 52–63.
Hailu, B.T., Maeda, E.E., Heiskanen, J., Pellikka, P., 2015. Reconstructing preagricultural expansion vegetation cover of Ethiopia. Appl. Geogr. 62, 357–365.
Haines, Y.R., 2009. Land use and biodiversity relationships. Land Use Pol. 26, 178–186.
Hansen, A.J., Defries, R., 2007. Ecological mechanisms linking protected areas to surrounding lands. Ecol. Appl. 17 (4), 974–988.
Hansen, M.C., Loveland, T.R., 2012. A review of large area monitoring of land cover change using Landsat data. Remote Sens. Environ. 122, 66–74.
Haregeweyn, N., Tesfaye, S., Tsunekawa, A., Tsubo, M., Meshesha, D., Adgo, E., Elias, A., 2015. Dynamics of land use and land cover and its effects on hydrologic responses: case study of the Gilgel Tekeze catchment in the highlands of Northern Ethiopia. Environ. Monit. Assess. 187, 4090.
Hartter, J., Southworth, J.D., 2009. Windling resources and fragmentation of landscapes around parks: wetlands and forest patches around Kibale National Park, Uganda. Landsc. Ecol. 24 (5), 643–656.
Hassan, Z., Shabbir, R., Ahmad, S.S., Malik, A.H., Aziz, N., Butt, A., Erum, S., 2016. Dynamics of land use and land cover change (LULCC) using geospatial techniques: a case study of Islamabad Pakistan. Springer Plus 5 (812), 11.
Hilker, T., Lyapustin, A.I., Tucker, C.J., Sellers, P.J., Hall, F.G., Wang, Y., 2012. Remote sensing of tropical ecosystems: atmospheric correction and cloud masking matter. Remote Sens. Environ. 127 (D18), 370–384.
Hisdal, L., Tallaksen, L.M., 2000. Drought event definition. Technical Report. In: Assessment of Regional Impacts of Droughts in Europe. University Oslo, Oslo, Norway.
Huang, S., Kong, J., 2016. Assessing land degradation dynamics and distinguishing human-induced changes from climate factors in the three-north shelter forest region of China. ISPRS Int. J. Geo-Inf. 5 (9), 158.

IBM Corp, 2019. IBM SPSS Statistics for Windows, Version 26.0. IBM Corp, Armonk, New York.
Jones, D.A., Hansen, A.J., Bly, K., Doherty, K., Verschuyl, J.P., Paugh, J.I., Story, S.J., 2009. Monitoring land use and cover around parks: a conceptual approach. Remote Sens. Environ. 113 (7), 1346–1356.
Jones, K.R., Venter, O., Fuller, R.A., Allan, J.R., Maxwell, S.L., Negret, P.J., et al., 2018. One-third of global protected land is under intense human pressure. Science 360, 788–791.
Kamga, M.A., Fils, S.C.N., Ayodele, M.O., Olatubara, C.O., Nzali, S., Adenikinju, A., Khalifa, M., 2020. Evaluation of land use/land cover changes due to gold mining activities from 1987 to 2017 using landsat imagery, East Cameroon. Geojournal 85, 1097–1114.
Kamwi, J.M., Chirwa, P.W.C., Manda, S.O.M., Graz, F.P., Katsch, C., 2015. Livelihoods, land use and land cover change in the Zambezi Region, Namibia. Popul. Environ. 36, 1–24.
Kamwi, J.M., Cho, M.A., Kaetsch, C., Manda, S.O., Graz, F.P., Chirwa, P.W., 2018. Assessing the spatial drivers of land use and land cover change in the protected and communal areas of the Zambezi region, Namibia. Land 7 (131), 13.
Karakas, C.B., Cerit, O., Kavak, K.S., 2015. Determination of land use land cover change and land use potentials of Sivas city and its surroundings using Geographical information systems and remote sensing. Procedia Earth Planet. Sci. 15, 454–461.
Karakus, C.B., Kavak, K.S., Cerit, O., 2014. Determination of variations in land cover and land use by remote sensing and geographic information systems around the city of Sivas (Turkey). Fresenius Environ. Bull. 23 (3), 667–677.
Kassa, T., Anton, V.R., Jean, P., Simon, V.B., Jozef, D., Kassa, A., 2014. Spatial analysis of land cover changes in eastern tigray, Ethiopia from 1965 to 2007: are there signs of a forest transition? Land Degrad. Dev.
Keesing, F., Belden, L.K., Daszak, P., Dobson, A., Harvell, C.D., Holt, R.D., Ostfeld, R.S., 2010. Impacts of biodiversity on the emergence and transmission of infectious diseases. Nature 468, 647–652.
Keshtkar, H., Voigt, W., Alizadeh, E., 2017. Land-cover classification and analysis of change using machine learning classifiers and multitemporal remote sensing imagery. Arabian J. Geosci. 10 (6).
Kindu, M., Schneider, T., Teketay, T., Knoke, T., 2015. Drivers of land use/land cover changes in Munessa-Shashemene landscape of the south-central highlands of Ethiopia. Environ. Monit. Assess. 187, 452.
Klimanova, O., Naumov, A., Greenfieldt, Y., Prado, R.B., Tretyachenko, D., 2018. Regional trends of land use and land cover transformation in Brazil in 2001-2012. Geogr. Environ. Sustain. 10 (4), 98–116.
Krauss, J., Bommarco, R., Guardiola, M., Heikkinen, R.K., Helm, A., Kuussaari, M., Steffan, D.I., 2010. Habitat fragmentation causes immediate and time-delayed biodiversity loss at different trophic levels. Ecol. Lett. 13, 597–605.
Lambin, E.F., Geist, H.J. (Eds.), 2006. Land Use and Land Cover Change: Local Processes and Global Impacts. Springer-Verlag, Heidelberg.
Lambin, E.F., Geist, H.J., Lepers, E., 2003. Dynamics of land use/cover change in tropical regions. Annu. Rev. Environ. Resour. 28, 205–241.
Lambin, E.F., Meyfroidt, P., 2010. Land use transitions: Socioecological feedback versus socioeconomic change. Land Use Pol. 27, 108–118.
Lambin, E.F., Turner, B.L., Geist, H.J., Agbola, S.M., Angelsen, A., Bruce, J.W., Coomes, O.T., Dirzo, R., Fischer, G., Folke, C., et al., 2001. The causes of land use/land cover change: moving beyond myths. Global Environ. Change 11, 261–269.
Lemenih, M., Kassa, H., Kassie, G.T., Damtew, A., Welday, T., 2014. Resettlement and woodland management problems and options: a case study from North-Western Ethiopia. Land Degrad. Dev. 25, 305–318.
Lepers, E., Lambin, E.F., Janetos, A.C., DeFries, R., Achard, F., Ramankutty, N., Scholes, R.J., 2005. A synthesis of information on rapid land-cover change for the period 1981-2000. Bioscience 55, 115–124.
Lesschen, J.P., Verburg, P.H., Staal, S.J., 2005. Statistical Methods for Analyzing the Spatial Dimension of Changes in Land Use and Farming Systems. International Livestock Research Institute, Nairobi, Wageningen, p. 80p.
Li, J., Lewis, J., Rowland, J., Tappan, G., Tieszen, L.L., 2004. Evaluation of land performance in Senegal using multitemporal NDVI and rainfall series. J. Arid Environ. 59, 463–480.
Li, X.Y., Ma, Y.J., Xu, H.Y., Wang, J.H., Zhang, D.S., 2009. Impact of land use and land cover change on environmental degradation in Lake Qinghai watershed, northeast of Qinghai-Tibet Plateau. Land Degrad. Dev. 20, 69–83.
Lillesand, T., Kiefer, R., Chipman, J., 2008. Remote Sensing and Image Interpretation, sixth ed. John Wiley and Sons, New York, USA, p. 756p.
Liu, C., Frazier, P., Kumar, L., 2007. Comparative assessment of the measures of thematic classification accuracy. Remote Sens. Environ. 107 (4), 606–616.
Lu, X., Zhou, Y., Liu, Y., LePage, Y., 2018. The roles of protected areas in land use land cover change and the carbon cycle in the conterminous United States. Global Change Biol. 24, 617–630.
Lung, T., Schaab, G.A., 2009. Comparative assessments of land cover dynamics of three protected forest areas in tropical eastern Africa. Environ. Monit. Assess. 161 (1-4), 531–548.
Maeda, E.E., Clark, B.J.F., Pellikka, P., Siljander, M., 2010. Modeling agricultural expansion in Kenya's Eastern Arc Mountains biodiversity hotspot. Agric. Syst. 103, 609–620.
Maina, J., Wandiga, S., Gyampoh, B., Charles, K.K.G., 2020. Assessment of land use and land cover change using GIS and remote sensing: a case study of Kieni, Central Kenya. J. Remote Sens. GIS 9, 270.
Maitima, J.M., Mugatha, S.M., Reid, R.S., Gachimbi, L.N., Majule, A., Lyaruu, H., Pomery, D., Mathai, S., Mugisha, S., 2009. The linkages between land use change, land degradation and biodiversity across East Africa. Afr. J. Environ. Sci. Technol. 3, 310–325.
Maitima, J.M., Olson, J.M., Mugatha, S.M., Mugisha, S., Mutie, T., 2010. Land use changes, impacts and options for sustaining productivity and livelihoods in the basin of lake Victoria. J. Sustain. Dev. Afr. 12, 3.
Mamude, M., Melka, G.A., Genet, W., 2021. Geospatial techniques based analysis on the impact of resettlement on land use and land cover change in Esira district, dawuro zone, Ethiopia. Ghana J. Geogr. 13 (1), 203–220.
Manandhar, R., Odeh, A.O.I., Ancev, T., 2009. Improving the accuracy of land use and land cover classification of landsat data using PostClassification enhancement. Remote Sens. 1 (3), 330–344.
Marchant, R., Richer, S., Boles, O., Capitani, C., Courtney-Mustaphi, C.J., Lane, P., Prendergast, M.E., Stump, D., De Cort, G., Kaplan, J.O., et al., 2018. Drivers and trajectories of land cover change in East Africa: human and environmental interactions from 6000 years ago to present. Earth Sci. Rev. 178, 322–378.
Martiny, N., Camberlin, P., Richard, Y., Philippon, N., 2006. Compared regimes of NDVI and rainfall in semiarid regions of Africa. Int. J. Remote Sens. 27 (23), 5201–5223.
Mekuyie, M., Jordaan, A., Melka, J., 2018. Land-use and land-cover changes & their drivers in rangeland-dependent pastoral communities in the southern Afar Region of Ethiopia. Afr. J. Range Forage Sci. 35, 33–43.
Meneses-Tovar, C.L., 2011. NDVI as indicator of degradation. Unasylva 238 (62), 40–46.
Mesfin, D., Simane, B., Belay, A., Recha, J.W., Taddese, H., 2020. Woodland cover change in the Central Rift Valley of Ethiopia. Forests 11 (916), 16p.
Mohamed, A.l., Anders, J., Schneider, C., 2020. Monitoring of changes in land use/land cover in Syria from 2010 to 2018 using multitemporal landsat imagery and GIS. Land 9 (226), 1–30.
Mohy, H., Abou El-Magd, I., Basta, F.F., 2016. Newly Improved Band Ratio of ASTER Data for Lithological Mapping of the Fawakhir Area, Central Eastern Desert, Egypt. Indian Soc. Remote Sens. 1–2.
Mota, A.A., Lachore, S.T., Handiso, Y.H., 2019. Assessment of food insecurity and its determinants in the rural households in Damot Gale Woreda, Wolaita zone, southern Ethiopia. Agric. Food Secur. 8 (1), 11.
Msigwa, A., Komakech, H.C., Verbeiren, B., Salvadore, E., Hessels, T., Weerasinghe, I., Griensven, A., 2019. Accounting for seasonal land use dynamics to improve estimation of agricultural irrigation water withdrawals. Water 11 (2471), 20.
Mtui, D.T., Lepczyk, C.A., Chen, Q., Miura, T., Cox, L.J., 2017. Assessing multidecadal land-cover -land-use change in two wildlife protected areas in Tanzania using Landsat imagery. PLoS One 12 (9), e0185468, 20p.
Mucova, S.A.R., Filho, W.L., Azeiteiro, U.M., Pereira, M.J., 2018. Assessment of land use and land cover changes (1979-2017) and biodiversity and land management approach in Quirimbas National Park, Northern Mozambique, Africa. Global Ecol. Conserv. 16 e00447, 17p.
Muhammed, A., Elias, E., 2021. Class and landscape level habitat fragmentation analysis in the Bale mountains national park, southeastern Ethiopia. Heliyon 7, e07642.
Munthali, M.G., Davis, N., Adeola, A.M., Botai, J.O., Kamwi, J.M., Chisale, H.L.W., 2019. Local perception of drivers of land-use and land-cover change dynamics across Dedza district, Central Malawi Region. Sustainability 11 (832), 25.
Musa, L., Peters, K., Ahmed, M., 2006. On farm characterization of Butana and Kenana cattle breed production systems in Sudan. Livest. Res. Rural Dev. 18, 1277–1288.
Mwavu, E.N., Witkowski, E.T., 2008. Land-use and cover changes (1988–2002) around Budongo forest reserve, NW Uganda: implications for forest and woodland sustainability. Land Degrad. Dev. 19, 606–622.
Naif, S.S., Mahmood, D.A., Al-Jiboori, M.H., 2020. Seasonal normalized difference vegetation index responses. Open Agric. 5, 631–637.
Nune, S., Soromessa, T., Teketay, D., 2016. Land use and land cover change in the Bale Mountain eco-region of Ethiopia during 1985 to 2015. Land 5 (41), 22.
Othow, O.O., Gebre, S.L., Gemeda, D.O., 2017. Analyzing the rate of land use/land cover change and determining the causes of forest cover change in Gog district, Gambella regional state, Ethiopia. J. Remote Sens. GIS 6 (4), 1–13.
Pei, Z., Fang, S., Yang, W., Wang, L., Wu, M., Zhang, Q., Han, W., Khoi, D.N., 2019. The relationship between NDVI and climate factors at different monthly time scales: a case study of grasslands in inner Mongolia, China (1982-2015). Sustainability 11 (7243), 1–17.
Prosper, L.B., Guan, Q., Cheng, D., 2015. Exploring land use and land cover change in the mining areas of wa East district, Ghana using satellite imagery. Open Geosci. 1, 618–626.
Rani, M.S., Schroth, O., Ross, C., et al., 2017. The effect of topographic correction on SPOT6 land cover classification in water catchment areas in Bandung Basin, Indonesia. In: GISRUK 2017 Proceeding. GISRUK 2017, 18-21 Apr 2017, Manchester, UK. Geographical Information Science Research UK, Manchester.
Rathnayake, C.W.M., Jones, S., Soto-Berelov, M., 2020. Mapping land cover change over a 25 Year period (1993-2018) in Sri Lanka using landsat time-series. Land 9 (27), 1–19.
Rawat, J.S., Biswas, V., Kumar, M., 2013. Changes in land use/land cover using geospatial techniques: a case study of Ramnagar town area, district Nainital Uttarakhand, India. Egypt. J. Remote Sens. Space Science 16, 111–117.
R-Development Core Team, 2019. R: A Language and Environment for Statistical Computing. R-Foundation for Statistical Computing, Vienna, Austria. https://www.r-project.org.
Rogan, J., Chen, D., 2004. Remote sensing technology for mapping and monitoring land cover and land-use change. Prog. Plann. 61, 301–325.
Sala, O.E., Chapin, F.S., Armesto, J.J., Berlow, E., Bloomfield, J., Dirzo, R., Wall, D.H., 2000. Global biodiversity scenarios for the year 2100, (New York). Science 287, 1770–1774.
Sancheza Reyes, U.J., Nino-Maldonado, S., Barrientos-Lozano, L., Trevino-Carreon, J., 2017. Assessment of land use-cover changes and Successional Stages of vegetation in the natural protected area Altas Cumbres, northeastern Mexico, using landsat satellite imagery. Remote Sens. 9 (712), 33p.

Sanz, E., Saa-Requejo, A., Díaz-Ambrona, C.H., Ruiz-Ramos, M., Rodríguez, A., Iglesias, P., et al., 2021. Normalized difference vegetation index temporal responses to temperature and precipitation in arid rangelands. Remote Sens. 13 (840), 1–24.

Schmitz, C., van Meijl, H., Kyle, P., Nelson, G.C., Fujimori, S., Gurgel, A., Havlik, P., Heyhoe, E., 2014. Land-use change trajectories up to 2050: insights from a global agro-economic model comparison. Agric. Econ. 45, 69–84.

Schnur, M.T., Hongjie, X., Wang, X., 2010. Estimating root zone soil moisture at distant sites using MODIS NDVI and EVI in a semiarid region of southwestern USA. Ecol. Inf. 5, 400–409.

Sharma, R., Nehren, U., Rahman, S.A., Meyer, M., Rimal, B., Seta, G.A., Baral, H., 2018. Modeling land use and land cover changes and their effects on biodiversity in central Kalimantan, Indonesia. Land 7 (57), 14.

Shoshani, J., Demeke, Y., 2008. Report on the Kafta Sheraro national park. In: Memorial to Professor Jeheskel Shoshani. Tigray Region, Ethiopia.

Sintayehu, D.W., Kassaw, M., 2019. Impact of land cover changes on elephant conservation in babile elephant sanctuary, Ethiopia. Biodivers. Int. J. 3 (2), 65–71.

Sleeter, B.M., Sohl, T.L., Bouchard, M.A., Reker, R.R., Soulard, C.E., Acevedo, W., Zhu, Z., 2012. Scenarios of land use and land cover change in the conterminous United States: utilizing the special report on emission scenarios at Eco regional scales. Global Environ. Change 22 (4), 896–914.

Smits, P.C., Dellepiane, S.G., Schowengerdt, R.A., 1999. Quality assessment of image classification algorithms for land-cover mapping: a review and proposal for a cost-based approach. Int. J. Remote Sens. 20, 1461–1486.

Solomon, B., Amsalu, A., Abebe, E., 2014. Land use and land cover changes in Awash national park, Ethiopia: impact of decentralization on the use and management of resources. Open J. Ecol. 4, 950–960.

Takala, W., Adugna, T., Miegel, K., 2020. Drivers and implications of land use/land cover dynamics in Finchaa catchment, northwestern Ethiopia. Land 9 (113), 1–20.

Tefera, M.M., 2011. Land-use/land-cover dynamics in Nonno district, central Ethiopia. J. Sustain. Dev. Afr. 13 (1), 123–141.

Tekle, K., Hedlund, L., 2000. Land cover changes between 1958 and 1986 in Kalu district, southern wello, Ethiopia. Mt. Res. Dev. 20 (1), 42–51.

Temesgen, F., Warkineh, B., 2020. Woody species Structure and Regeneration status in Kafta Sheraro national park dry forest, tigray region, Ethiopia. Int. J. Financ. Res. 2020, 1–22. Article ID 4597456.

Viedma, O., Moreno, J.m., Rieiro, I., 2006. Interaction between land use/land cover change, forest fires and land scape structure in Sierrra de Gredos (central Spain). Environ. Conserv. 33 (3), 212–222.

Vreugdenhil, D., Vreugdenhil, A.D., Tilahun, T., Shimelis, A., Tefera, Z., 2012. Gap Analysis of the Protected Areas System of Ethiopia, with Technical Contributions from Nagelkerke, L., Gedeon, K., Spawls, S., Yalden,D., Lakew Berhanu, and Siege, L. World Institute for Conservation and Environment, USA, p. 68.

Wang, Y., Dai, E., Yin, L., Ma, L., 2018. Land use/land cover change and the effects on ecosystem services in the Hengduan Mountain region, China. Ecosyst. Serv. 1 (34), 55–67.

Wilson, S.A., Wilson, C.O., 2012. Modeling the impacts of civil war on land use and land cover change within Kono District, Sierra Leone: a sociogeospatial approach. Geocarto Int. 1–26.

Xia, J., Liu, S., Liang, S., Chen, Y., Xu, W., Yuan, W., 2014. Spatiotemporal patterns and climate variables controlling of biomass carbon stock of global grassland ecosystems from 1982 to 2006. Remote Sens. 6, 1783–1802.

Yadeta, T., Deribew, K.T., Getahun, K., Debesa, G., Abreha, G., Hailu, S., 2022. Recent resettlement programs, as drivers for Afromontane forest loss in the Hawa-Galan district of Ethiopia. Cogent Social Sci. 8 (1), 2088462.

Young, J., 2012. Ethiopian Protected Areas: A 'Snapshot'. A Reference Guide for Future Strategic Planning and Project Funding, Addis Abeba, Ethiopia, p. 46.

Zewdie, W., Csaplovics, E., 2016. Identifying Categorical land use transition and land degradation in north western drylands of Ethiopia. Remote Sens. 8 (408), 20.

Zhao, F., Xu, B., Yang, X., Jin, Y., Li, J., Xia, L., Chen, S., Ma, H., 2014. Remote sensing estimates of grassland aboveground biomass based on MODIS Net Primary Productivity (NPP): a case study in the Xilingol Grassland of northern China. Remote Sens. 6, 5368–5386.